THE UNIVERSITY of EDINBURGH

Edinburgh Research Explorer

Detrital zircon U-Pb ages in the Rif Belt (northern Morocco): Paleogeographic implications

Citation for published version:
Azdimousa, A, Jabaloy-sánchez, A, Talavera, C, Asebriy, L, González-lodeiro, F & Evans, NJ 2019, 'Detrital zircon U-Pb ages in the Rif Belt (northern Morocco): Paleogeographic implications', *Gondwana Research*, vol. 70, pp. 133-150. https://doi.org/10.1016/j.gr.2018.12.008

Digital Object Identifier (DOI):
10.1016/j.gr.2018.12.008

Link:
Link to publication record in Edinburgh Research Explorer

Document Version:
Peer reviewed version

Published In:
Gondwana Research

General rights
Copyright for the publications made accessible via the Edinburgh Research Explorer is retained by the author(s) and / or other copyright owners and it is a condition of accessing these publications that users recognise and abide by the legal requirements associated with these rights.

Take down policy
The University of Edinburgh has made every reasonable effort to ensure that Edinburgh Research Explorer content complies with UK legislation. If you believe that the public display of this file breaches copyright please contact openaccess@ed.ac.uk providing details, and we will remove access to the work immediately and investigate your claim.

OPEN ACCESS

Download date: 13. May. 2024

Accepted Manuscript

Detrital zircon U-Pb ages in the Rif belt (northern Morocco): Paleogeographic implications

Ali Azdimousa, Antonio Jabaloy-Sánchez, Cristina Talavera, Lahcen Asebriy, Francisco González-Lodeiro, Noreen J. Evans

PII:	S1342-937X(19)30024-3
DOI:	https://doi.org/10.1016/j.gr.2018.12.008
Reference:	GR 2080
To appear in:	*Gondwana Research*
Received date:	19 May 2018
Revised date:	20 November 2018
Accepted date:	2 December 2018

Please cite this article as: A. Azdimousa, A. Jabaloy-Sánchez, C. Talavera, et al., Detrital zircon U-Pb ages in the Rif belt (northern Morocco): Paleogeographic implications, Gondwana Research, https://doi.org/10.1016/j.gr.2018.12.008

This is a PDF file of an unedited manuscript that has been accepted for publication. As a service to our customers we are providing this early version of the manuscript. The manuscript will undergo copyediting, typesetting, and review of the resulting proof before it is published in its final form. Please note that during the production process errors may be discovered which could affect the content, and all legal disclaimers that apply to the journal pertain.

ACCEPTED MANUSCRIPT

Detrital zircon U–Pb ages in the Rif Belt (northern Morocco): Paleogeographic implications

Ali Azdimousa[1]; Antonio Jabaloy-Sánchez[2], Cristina Talavera[3,4]; Lahcen Asebriy[5]; Francisco González-Lodeiro[6], Noreen J. Evans[4,7]

[1]Faculté Pluridisciplinaire de Nador & Laboratoire des Géosciences Appliquées, Faculté des Sciences, Université Mohammed I, Oujda, Morocco.

[2]Department of Geodynamics, University of Granada, Granada, Spain

[3]School of Geosciences, University of Edinburgh, The King's Building, James Hutton Road, EH9 3FE, Edinburgh, UK

[4]John de Laeter Center, Curtin University, Bentley 6845, Australia

[5]Laboratoire de Géo-biodiversité et du Patrimoine Naturel (GEOBIO), Centre de Recherche "Geophysics, Natural Patrimony and Green Chemistry" (GEOPAC), Institut Scientifique, Université Mohammed V de Rabat, Morocco

[6]Instituto Geológico y Minero de España, Madrid, Spain

[7]School of Earth and Planetary Science, Curtin University, Perth, WA, Australia

ACCEPTED MANUSCRIPT

Abstract

Detrital zircon U-Pb age distributions in Mesozoic and Cenozoic rocks from the External Rif and Maghrebian Flysch Complex (including the so-called Mauretanian internal flysch units) are very similar, strongly suggesting that the External Rif and the entire Maghrebian Flysch Complex were part of the same NW African paleomargin. These patterns include scarce Paleozoic zircon grains that show influence from the

ACCEPTED MANUSCRIPT

Sehoul block. Neoproterozoic and Paleoproterozoic grains are abundant with a dominant Ediacaran zircon population at ca. 590 Ma, which could have been sourced from the Variscan Moroccan Mesetas, the northern components of the West African Craton, or from Triassic sediments from the Central High Atlas and Argana basins. Mesoproterozoic zircon ages between 1.1 and 1.6 Ga were also observed (15 % in the combined age spectra), the nearest sources for these being in the central part of the West African Craton. Transport of the Mesoproterozoic grains to the NW African paleomargin requires northward-directed fluvial systems parallel to the Central Atlantic continental margin of Africa. In contrast, samples from the Internal Rif or Alborán Domain are different to those from the External Rif and Maghrebian Flysch Complex, especially in the scarcity of Mesoproterozoic zircons, suggesting that the Alborán Domain was not a source area for zircons found in the NW African paleomargin.

1. Introduction

The Rif Belt (North Western Africa, Fig. 1A and B) is a key area for understanding the relationship between the Central Atlantic and Neotethys oceans, and the closure of the Neotethys, which culminated in formation of the Western Mediterranean area and related Alpine orogenic belts. The U–Pb age of zircon grains from detrital deposits can provide valuable insights into orogenic evolution by constraining the maximum depositional age for these sedimentary units and informing 'source to sink' provenance.

However, these studies are scarce in the Rif belt area and existing work utilized a limited sample set. For example, Pratt et al. (2105) studied two samples from the Rif Belt and Marzoli et al. (2017) analysed a small number of samples from the Triassic

ACCEPTED MANUSCRIPT

rocks of the High Atlas. In this paper we present U–Pb zircon ages for seventeen samples of sedimentary quartzite from the Rif Belt (NW Africa), obtained using laser ablation inductively coupled plasma mass spectrometry (LA-ICP-MS). These data allow us to gain insights into the source areas and paleogeography of the different domains during orogenic belt evolution.

2. Geological setting

The Rif Belt and the Betic Cordillera form the southern and northern branches of the Gibraltar Arc, respectively, and together with the Tell and Calabrian-Peloritan Arc, constitute the extension of the Alpine orogenic belt in the southern part of the Western Mediterranean area (Fig. 1A). The Gibraltar Arc formed by several processes that include: i) closure of the Ligurian-Maghrebian Neotethys ocean; ii) spreading of the present-day Western Mediterranean oceanic crust; iii) collision of exotic continental terranes against the paleomargins of NW Africa, Iberian Peninsula and Apulia; iv) convergence between the African and Eurasian plates (Dewey et al., 1989; Jolivet et al., 2003; Chalouan et al., 2008).

Three main structural domains form the Rif Belt (Fig. 1B), from south to north: (i) the *External Rif*, (ii) *Maghrebian Flysch Complex*, and (iii) the *Internal Rif* or *Alborán Domain* (Fig. 1B). Each domain consists of tectonic complexes of stacked units.

2.1 The External Rif

ACCEPTED MANUSCRIPT

The lithologic units in the External Rif are interpreted as being the product of deformation and partial metamorphosis of the NW African paleomargin, overthrust by the Maghrebian Flysch Complex and the units of the Internal Rif. This region is primarily comprised of Mesozoic and Cenozoic sediments, and includes minor mafic and ultramafic bodies (Lespinasse, 1975; Asebriy, 1984; Ciszak et al., 1986; Asebriy et al., 1987; Ciszak, 1987; Kuhnt and Obert, 1991).

The rocks of the External Rif (Figs. 2 and 3) are grouped into two structural units: the Sub-Rif units and Pre-Rif units (Asebriy et al., 1987). The Pre-Rif units, to the south of the Rif Belt, comprise the outermost zone of the External Rif, with a frontal fold-and-thrust belt including a series of thin Jurassic and Lower Cretaceous successions detached from the Paleozoic basement ("Rides Prérifaines", see Michard, 1976; Ben Yaïch, 1991; Favre, 1992). The "Rides Prérifaines" are overthrust by a sedimentary complex composed of Paleozoic to Cenozoic blocks in a matrix of Tortonian marls ("Nappe Prérifaine", Levy and Tilloy, 1952; Vidal, 1971; Leblanc, 1975-1979; Bourgois, 1977; Suter, 1980; Feinberg, 1986; Kerzazi, 1994) (Fig. 3).

The Sub-Rif units (Asebriy et al., 1987) include the so-called Intra-Rif and Meso-Rif zones as defined by Durand-Delga et al. (1962, see Chalouan et al, 2008). The Sub-Rif units are composed of diagenetic to low-grade metamorphic rocks deformed under ductile to brittle conditions (Andrieux, 1971; Frizon de Lamotte, 1985; Michard et al., 1992; Asebriy, 1994; Asebriy et al., 2003; Azdimousa et al., 1998, 2007) (Figs. 1B and 2). In the eastern Rif Belt, the Sub-Rif units comprise several groups of tectonic units, from bottom to top: i) Temsamane units; ii) Tanger-Ketama unit; iii) Aknoul units (Fig. 2).

2.1.2 The Temsamane units

ACCEPTED MANUSCRIPT

The Temsamane units comprise the basement of the Eastern Meseta and its Mesozoic cover, and have been affected by Alpine metamorphism and deformation to form a fold-and-thrust stack. The Alpine ductile deformation generated a strong planar-linear fabric with an ENE-WSW trending stretch lineation under a WSW sense of shearing (Frizon de Lamotte, 1985, 1987a, b; Jabaloy et al., 2015; Azdimousa et al., in press).

The uppermost Temsamane unit is the so-called Ras Afraou unit, which is composed of chloritoid-bearing black schists usually attributed to the Paleozoic (See Negro, 2005; Azdimousa et al., 2007, in press, and Negro et al., 2007, and references therein), and is covered by whitish marbles attributed to the Jurassic (see Jabaloy et al., 2015) (Fig. 4).

The lithological succession below the Ras Afraou unit begins with Paleozoic dark schists and quartzites (Fig. 4). A nearly continuous layer of Triassic metabasites, metamorphosed to greenschists facies, overlays the Paleozoic rocks, and these are in turn covered by Jurassic calcitic and dolomitic marbles. Moving up section, there are Berriasian-Barremian whitish phyllites and shales, alternating with marbles which are overlaid by Aptian-Lower Albian black phyllites and shales alternating with quartzites (Azdimousa et al., 2007) (Fig. 4).

Negro (2005) and Negro et al. (2007) estimated the metamorphic P-T conditions of the chloritoid-bearing black schists of the Ras Afraou unit at 350 ± 30 °C and 7-8 kbars. The Temsamane units outcrop in the southern part of the belt and experienced lower P-T conditions ranging from late diagenesis in the south, to epizone in the north (Jabaloy et al., 2015). $^{40}Ar/^{39}Ar$ radiometric ages on white micas indicate Chattian to Langhian ages for the metamorphism (Monie et al., 1984; Negro et al., 2008; Jabaloy et al., 2015).

ACCEPTED MANUSCRIPT

2.1.2 The Tanger-Ketama unit

The Tanger-Ketama unit includes two different types of substratum below the Lower Cretaceous rocks (see Chalouan et al., 2008; Vázquez et al., 2013). In the western and central outcrops of the unit, the Lower Cretaceous sediments cover ≈500 m of Jurassic carbonate and pelitic sedimentary rocks (Asebriy et al., 1992, Asebriy, 1994) (Fig. 4). The Jurassic succession includes Sinemurian massive limestones, covered by ammonite-rich marly limestones (Ammonitico Rosso facies, Pliensbachian), silty marls (Toarcian), hemipelagic limestones rich in filaments (Aalenian), and Posidonomya marls. Up section, there is the "ferrysch" (an Amazigh word for a rhythmic deposit of alternating marls and sandstones) of Callovian to Oxfordian age, overlain by Tithonian-Berriasian pelagic limestones (Asebriy et al., 1992, Asebriy, 1994).

In the eastern outcrops, the Lower Cretaceous sedimentary rocks overlay the ultramafic rocks of the Beni-Malek massif, which consist of partially serpentinised spinel lherzolites (Michard et al., 1992). Michard et al. (1992), Chalouan et al. (2008), and Vázquez et al. (2013) interpreted the Beni-Malek ultramafic body as a sliver of serpentinized mantle, exposed on the sea floor during rifting in a non-volcanic continental margin.

Covering both substrates, there is a succession of carbonate shales with limestones and sandstones dated as Berriasian-Hauterivian. Further up section there is a 500 metre thick sequence of Aptian-Lower Albian dark shales and thick quartzitic turbidites (the so-called Black Flysch, see Frizon de Lamotte, 1985, and also Asebriy et al., 1992, Azdimousa et al., 1998; 2003) (Fig. 4). Uppermost Albian marls and spongolites are preserved to the north of the outcrops (Asebriy et al., 1992).

ACCEPTED MANUSCRIPT

The Upper Cretaceous to Neogene succession of the Tanger-Ketama Unit is called the Tanger Unit when it is partly detached from the underlying Lower Cretaceous rocks. The Tanger succession begins with about 50 meters of Uppermost Albian green pelites, followed by about 600 m of Late Cretaceous to Paleocene pelitic and carbonate formations (see Zaghloul et al., 2005, and references therein) (Fig. 4). The succession continues with ca. 50 m of Late Paleocene-Early Eocene marls with black flint, covered by ca. 100 m of Middle Eocene to Middle Miocene marls and turbiditic sandstones (Zaghloul et al., 2005) (Fig. 4). The same Upper Cretaceous to Neogene succession corresponds to the so-called Aknoul unit when it is completely detached from the Tanger-Ketama unit on top of the Cenomanian pelites and slides on top of both the Tanger-Ketama and the Temsamane units.

2.2 The Maghrebian Flysch Complex

The Maghrebian Flysch units extend from the Betic Cordillera to the Rif, Tell, Sicily, Calabria and the southern-central Apennines (e.g. Guerrera et al. 2012, and references therein). The successions of the Maghrebian Flysch are mainly made up of turbiditic siliciclastic (and subordinately carbonate) sandstones interlayered with clays, deposited in a very deep marine environment (slope/rise and abyssal plain). The age of these successions ranges between Early Cretaceous and Early Burdigalian. The successions are systematically detached from their original substratum, oceanic crust represented by Middle-Upper Jurassic basalts with E-MORB tendency, associated with Middle-Upper Jurassic radiolarites (Durand Delga et al., 2000).

Based on the proximity to the North African paleomargin, tectonic-paleogeographic nomenclature frequently used for the Maghrebian Flysch units

ACCEPTED MANUSCRIPT

separates the "external units" or "Massylian units" from the "internal units" or "Mauretanian units" near the Alborán Domain paleomargin. In the eastern and central Rif, they include: i) an external Massylian unit (Chouamat-Meloussa unit), related to ii) the external Numidian Fm or Numidian sandstones, and separated from iii) the internal Mauretanian units (Tisiren and Beni Ider units) (see Bouillin et al., 1970; Esteras et al., 2004; Durand Delga, 2006; Chalouan et al., 2008; Guerrera et al., 2012; Guerrera and Martín-Martín, 2014, and references therein),

The Massylian Flysch units are represented by the Chouamat-Meloussa succession, a thin tectonic sequence thrusted over the Tanger-Ketama unit. The Chouamat-Meloussa succession begins with a 700 m thick Aptian-Albian siliciclastic flysch, followed upward by thin black cherts and calcareous microbreccias (Cenomanian-Turonian), in turn overlain by Senonian pelites and microbreccias (Fig. 4).

The Numidian Formation is essentially a > 1 km thick succession of Latest Oligocene to Aquitanian ultra-mature quartz arenites associated with mainly kaolinitic pelites (Guerrera, 1981-1982; Guerrera and Puglisi, 1984; Fildes et al., 2010; Guerrera et al., 1993, 2012). It is considered to be the detached Cenozoic part of the Massylian succession (Esteras et al., 2004; Guerrera et al., 2012, and references therein) (Fig. 4). The Numidian sandstones were deposited by high-density turbidity currents and sand flows within enormous sand-rich deep clastic systems, located in the continental rise of the North African paleomargin (Pendón, 1977; Didon and Hoyez, 1978; Martín-Algarra, 1987; Hoyez, 1989; Guerrera et al., 2012). This turbiditic succession is overlain by brownish supra-Numidian clays dated as Latest Aquitanian-Middle Burdigalian (Guerrera et al., 2012).

ACCEPTED MANUSCRIPT

The internal Mauretanian strata include the Upper Jurassic to Lower Cretaceous Tisiren unit. The Tisiren succession is composed of, from bottom to top, thin Upper Jurassic radiolarites, marly limestones (Preflysch I, Berriasian-Valanginian), siliciclastic layers interlayered with Hauterivian-Barremian black shales related to a turbiditic episode (Sandstone episode I, see Durand Delga et al., 1999), a dominantly pelitic sequence (Preflysch II, Barremian-Early Aptian) and a new turbiditic episode (Sandstone episode II, Late Aptian-Middle Albian) (Fig. 4). The Mauretanian Beni Ider Unit is also found in the western Rif. It represents the detached upper part of the Tisiren unit and is formed of Upper Albian to Middle Burdigalian rocks with fragments of rocks and fossils indicating proximity to the Internal Alborán Domain.

2.3 The Internal Rif or Alborán Domain

The Internal Rif is part of the Alborán Domain according to Balanyá and García-Dueñas (1987). This Internal Rif has been interpreted as part of an allochthonous terrane formed by a stack of hinterland metamorphic units (Andrieux et al., 1971; Balanyá and García-Dueñas, 1987) that underwent subduction-collision processes (e.g. Azañón and Crespo-Blanc, 2000; Faccenna et al., 2004; Michard et al., 2006; Booth-Rea *et al.*, 2007). Similar exotic terranes are recognised in the Algerian Kabylides, Peloritan Mountains of Sicily, and in Calabria, and were supposedly part of the same continental domain (AlKaPeCa; Bouillin, 1984) before being deformed and dispersed. The initial location of AlKaPeCa is controversial as this domain may correspond to either a distal part of the Iberian margin (e.g. Chalouan et al., 2008), or an isolated microcontinent within the western Tethys (e.g. Guerrera et al., 2012).

ACCEPTED MANUSCRIPT

The Alborán Domain is composed of a lower Sebtide/Alpujárride Complex affected by HP-LT Alpine metamorphism, an upper Ghomaride/Maláguide Complex, which underwent diagenesis to very low grade Alpine metamorphism, and a set of sedimentary Frontal Units. The lower Sebtide/Alpujárride Complex comprises a mostly metapelitic Paleozoic basement covered by a Permian-Early Triassic Meta-detrital Fm of quartzites and phyllites, followed up section by a Middle-Late Triassic Meta-carbonate Fm of calcitic and dolomitic marbles. The upper Ghomaride/Maláguide Complex is composed of, from bottom to top, Paleozoic basement of Late Ordovician phyllites with interleaved quartzite and meta-conglomerates, Silurian phyllites including carbonate beds and black graptolite-bearing cherts, Early Devonian pillow basalts, black cherts and limestones, Devonian distal calci-turbidites, and unconformable Carboniferous pelites graywackes and conglomerates with Culm facies. The Paleozoic basement is covered by a Mesozoic-Cenozoic sedimentary succession.

3. Sampling localities

Seventeen samples from the Rif chain were studied, including seven samples from the Temsamane units: one sample from the upper Ras Afraou unit (Ri35), and six samples from the Aptian-Lower Albian quartzites (TEM5, TEM6, TEM7, BMK3, Ri66, and Ri68) (see Table 1). There also are five samples from the Tanger-Ketama unit: two from the Jurassic sandstones from the “Ferrysch”, two from the Aptian-Lower Albian Black Flysch, and one from the Middle Eocene to Middle Miocene rocks of the Tanger unit.

There are three samples from the Maghrebian Flysch units: two from the Lower Cretaceous Mauretanian Tisiren unit, (Ri111 and Ri117, Table 1), and one from the

ACCEPTED MANUSCRIPT

Numidian Fm. (Ri64, Table 1). For comparison, we have processed two samples from the Alborán Domain: Ri119 (Table 1) from the Paleozoic basement of the South Federico Unit of the Sebtide/Alpujárride Complex, and Ri121 (Table 1) from a sandstone within the Carboniferous rocks of the Akaili tectonic unit of the Ghomaride/Maláguide Complex.

4. Analytical Methods

4.1 Mineral separation and Cathodoluminescence images

Zircons were separated using standard heavy-liquid and magnetic techniques in the Department of Geodynamics of the University of Granada. Grains were handpicked and mounted in epoxy, polished, cleaned and gold coated for cathodoluminescence (CL) imaging on a Mira3 FESEM instrument at the John de Laeter Centre (JdLC), Curtin University, Perth, Australia. Representative CL images (Fig. 5) display lower-U regions as brightly illuminated regions and higher-U regions as dark, or even black, poorly illuminated regions.

4.2 LA-ICPMS methods

LA-ICP-MS data collection was performed at the GeoHistory Facility, JdLC, Curtin University, Perth, Australia. Following two cleaning pulses and 30 s of baseline acquisition, individual zircon grains (mounted and polished in 1" epoxy rounds) were ablated for 30 s using a Resonetics RESOlution M-50A-LR, incorporating a Compex 102 excimer laser, with a 33 μm diameter laser spot, 7 Hz laser repetition rate, laser

ACCEPTED MANUSCRIPT

energy of 1.8 J cm-2. The sample cell was flushed with ultrahigh purity He (350 mL min-1) and N_2 (3.6 mL min-1), both of which were passed through an inline Hg trap. High purity Ar was used as the plasma gas (flow rate 1 L min-1). Isotopic intensities were measured using an Agilent 7700 quadrupole ICP-MS and following elements were monitored for 0.03 s each: ^{28}Si, ^{29}Si, ^{49}Ti, ^{91}Sr, ^{147}Sm, ^{202}Hg, ^{204}Pb, ^{206}Pb, ^{207}Pb, ^{208}Pb, ^{232}Th, and ^{238}U. International glass standard NIST 610 was used as the primary standard to calculate elemental concentrations (using ^{29}Si as the internal standard element and assuming 14.76% Zr in unknowns) and to correct for instrument drift.

The primary age reference used in this study was GJ-1 (609 Ma; Jackson et al., 2004), with 91500 (1062.4±0.4 Ma; Wiedenbeck et al., 1995), Plesovice (337.13±0.37 Ma; Sláma et al., 2008) and OGC (3465.4 ± 0.6 Ma; Stern et al., 2009) used as secondary age standards. ^{206}Pb/^{238}U and ^{207}Pb/^{206}Pb ages calculated for all zircon age standards, treated as unknowns, were found to be within 3% of the accepted value. The time-resolved mass spectra were reduced using the Trace Elements and U_Pb_Geochronology3 data reduction schemes in Iolite (Paton et al, 2011 and references therein).

Errors cited for individual analyses are at the 2σ level. Dates for which the concordant values were > 110% or < 90% were considered to be excessively discordant and were not considered in the age discussion or plotted on the Wetherill Concordia diagrams. However, they are listed on Tables 2-5 (See Supplementary material). Weighted mean values for ages are based on pooled analyses and are provided at the 95% confidence level. Ages in the text and figures are quoted as ^{206}Pb/^{238}U dates for zircons younger than 1500 Ma and as ^{207}Pb/^{206}Pb dates for zircons older than 1500 Ma.

5. Results

ACCEPTED MANUSCRIPT

The CL images for representative zircon grains from each sample are provided in Fig. 5. The U-Pb data for individual samples (Tables A1 to A4 in Supplementary material), representative Concordia plots, and youngest zircon populations are in the Supplementary material (Figs. A1 to A8 in the Supplementary material), while their probability density plots age given in Figures 6 to 12 below.

5.1 Temsamane units

5.1.1 Lower Cretaceous quartzites alternating with dark phyllites

Six samples of quartzite from this unit were analysed (TEM5, TEM6, TEM7, BMK3, Ri66, and Ri68, Table 1). The separated zircons show a variety of morphologies and textures, but CL images show that most zircon grains have continuous oscillatory zoning (Fig. 5). There are also some structureless grains, grains with sector zoning, and grains with cores overgrown by low or high U rims (Fig. 5).

All six samples from the Aptian-Lower Albian quartzites (Fig. 6, and Table A1 in Supplementary material) and the combined data for the Temsamane units (807 U-Pb dates) show a very similar pattern of zircon age distribution (Fig. 7) with very scarce Mesozoic zircon grains. There are only two Middle-Upper Triassic grains (samples BKM3 and Ri68: 234 ± 3 Ma and 227 ± 10 Ma respectively). There are 57 Paleozoic grains (between 6 and 10 % on each sample), including 16 Upper Ordovician to Devonian (ca. 360-460 Ma), and 33 Cambrian to Middle Ordovician zircon grains (ca. 540-460).

Neoproterozoic dates are the most abundant, representing 45 to 60 % of all analysed grains. Most are Ediacaran with several peaks at ca. 556 and 597 Ma (Fig. 7). All samples contain between 10 and 19% Mesoproterozoic zircon grains, and from 18

ACCEPTED MANUSCRIPT

to 27% Paleoproterozoic zircon grains (Fig. 7). There are also Neoarchean (2.5%), Mesoarchean (2%), Paleoarchean (~0.2%) and Eoarchean (~0.1%) dates (Fig. 7).

The youngest population in four of these six samples is placed at the Ediacaran-Cambrian boundary (ca. 538-561 Ma). In the other two samples, the youngest population is either Ediacaran (ca. 561 Ma) or Cambrian (ca. 524 Ma) in age (Fig. A2 in the Supplementary material).

5.1.2 Black schists and quartzites of the upper Ras Afraou unit (Sample Ri-35)

Approximately 250 zircon grains with different textures and morphologies were handpicked from the Ri-35zircon concentrate. From the CL imaging, most of these zircons show continuous oscillatory zoning (Fig. 5). There are also some composite grains with cores overgrown by wide rims and some zircons with sector zoning (Fig. 5).

One hundred and fifty one analyses were performed on 148 zircons yielding 129 concordant ages ranging from 200 to 3009 Ma (Fig. 8, and Table A1in the Supplementary material). The distribution of concordant dates contrasts to that obtained on the Temsamane units described above with Mesozoic (8%), Paleozoic (57%), Neoproterozoic (18%), Mesoproterozoic (2%), Paleoproterozoic (12%), Neoarchean (2%) and Mesoarchean (1%) grains in 5 key populations at ca. 243, 270, 320, 583 and 2140 Ma (Fig. 8). The youngest zircon grain from this quartzite has a $^{206}Pb/^{238}U$ date of 200 ± 7 Ma (Table A1 in Supplementary material) and the youngest zircon population comprises eight dates with a $^{206}Pb/^{238}U$ age of 243 ± 3 Ma (MSWD = 1.02 and probability = 0.41) (Fig. A3 in Supplementary material).

5.2 Tanger-Ketama unit

ACCEPTED MANUSCRIPT

5.2.1 Jurassic sandstones from the "Ferrysch"

The CL images indicate that samples Ri102 and Ri107 contain zircon grains that have either continuous oscillatory zoning, sector zoning or are structureless (Fig. 5). There are also some composite zircons with partially resorbed cores overgrown by younger rims. The cores are structureless or display either oscillatory or sector zoning, and the rims are structureless or have weak oscillatory zoning (Fig. 5).

Ri102 and Ri107 (Fig. A8, and Table A2 in the Supplementary material) yield 223 concordant zircon ages ranging from 261 Ma to 3005 Ma with Paleozoic (10%), Neoproterozoic (45%), Mesoproterozoic (15%), Paleoproterozoic (24%), Neoarchean (5%) and Mesoarchean (1%) grains (Fig. 9). The youngest $^{206}Pb/^{238}U$ zircon date is 261 ± 28 Ma (Table A2 in the Supplementary material). The zircon age distribution is similar to the previously described Lower Cretaceous rocks of the Temsamane units (Fig. 9). There is a dominant Ediacaran population at ca. 591 Ma with a lower percentage of Cryogenian-Tonian grains, and an important component of Mesoproterozoic zircon grains (15%) (Fig. 9).

5.2.2 Lower Cretaceous quartzites of the Black Flysch

The zircons from samples Ri43 and Ri114 show the same structures in CL images as those previously described from the Jurassic samples: grains with either continuous oscillatory zoning, sector zoning, or no zoning (Fig. 5). There are also some composite zircons with partially resorbed cores overgrown by low or high U rims (Fig. 5).

The two samples from the Aptian-Lower Albian quartzites of the Black Flysch (Fig. 9, and Table A2 in the Supplementary material) yielded 275 concordant zircon ages ranging from 21 and 3244 Ma, with Cenozoic (0.4%), Mesozoic (0.4%) Paleozoic

ACCEPTED MANUSCRIPT

(9%), Neoproterozoic (40%), Mesoproterozoic (15%), Paleoproterozoic (30%), Neoarchean (3%), Mesoarchean (2%), and Paleoarchean grains (0.4%) (Fig. 9). The youngest zircon from this sample has a $^{206}Pb/^{238}U$ date of 21 ± 6 Ma (Table A2 in the Supplementary material). The detrital zircon age distributions are very similar to the previously described ages patterns with a dominant Ediacaran population with a peak at ca. 597 Ma, and secondary Mesoproterozoic (at ca. 1181 and 1445 Ma) and Paleoproterozoic peaks (at ca. 1871, 1980 and 2114 Ma, Fig. 9).

5.2.3 Sandstones with Middle Eocene to Middle Miocene ages from the Tanger unit

Sample Ri63

Approximately 60 zircons with different textures, morphologies, sizes and colours were handpicked from the zircon concentrate of this sandstone. These zircons mainly show continuous oscillatory zoning (Fig. 5) although there a few composite grains with a partially resorbed core overgrown by a rim (Fig. 5).

Fifty five analyses were performed on 48 zircons, 46 of which yielded concordant or nearly concordant dates ranging from 413 to 2590 Ma (Fig. 10, and Table A2 in the Supplementary material). The populations are Paleozoic (9%), Neoproterozoic (41%), Mesoproterozoic (15%), Paleoproterozoic (31%) and Neoarchean (4%) and cluster in three main groups at ca. 627, 1041 and 1945 Ma (Fig. 10). The youngest zircon of this quartzite has $^{206}Pb/^{238}U$ date of 413 ± 17 Ma (Table A2 in the Supplementary material) and the youngest zircon population composed of four dates has a $^{206}Pb/^{238}U$ mean age of 598 ± 11 Ma (MSWD = 1.3 and probability = 0.29) (Fig. A6 in the Supplementary material).

5.3 Maghrebian Flysch units

ACCEPTED MANUSCRIPT

5.3.1 Lower Cretaceous Sandstones from the Mauretanian Tisiren Unit

Two samples from the Tisiren Flysch were processed (Ri111 and Ri117). Sample Ri117 contains abundant zircon grains that show either continuous oscillatory zoning or sector zoning in CL images (Fig. 5), however some grains are structureless. There are also partially resorbed cores overgrown by mainly thin low or high U rims (Fig. 5). On the other hand, sample Ri111 had scarce zircon grains and the CL images show only zircon grains with continuous oscillatory zoning (Fig. 5). No inherited cores were distinguished (Fig. 5).

The two samples (Fig. 11, and Table A3 in the Supplementary material) yielded 138 concordant ages ranging from 293 to 2772 Ma, with Paleozoic (7%), Neoproterozoic (48%), Mesoproterozoic (15%), Paleoproterozoic (28%), and Neoarchean (2%) dates. They are grouped into four main populations at ca. 528, 599, 2103 and 2188 Ma (Fig. 11). These samples also have a similar age distribution to the previously described Mesozoic samples from the Temsamane and the Tanger-Ketama units.

5.3.2 Latest Oligocene to Aquitanian quartzite arenite from the Numidian Fm

Sample Ri64

The CL images show that most zircons from Ri64 have continuous oscillatory zoning and only a few grains display sector zoning or are structureless (Fig. 5). There are also some composite zircons with partially resorbed cores overgrown by thick rims (Fig. 5).

One hundred and fifty analyses were performed on 140 zircons, all of which yielded concordant or nearly concordant dates (Fig. 10 and Table A3 in the

ACCEPTED MANUSCRIPT

Supplementary material). These dates range from 347 Ma to 2888 Ma, are Paleozoic (5%), Neoproterozoic (49%), Mesoproterozoic (9%), Paleoproterozoic (31%), Neoarchean (5%) and Mesoarchean (1%) in age, and cluster in five main populations at ca. 597, 656, 1744, 1893 and 2054 Ma (Fig. 10). The youngest $^{206}Pb/^{238}U$ zircon date is 347 ± 6 Ma (Table A3 in the Supplementary material) and the youngest zircon population, comprising 14 dates, has a $^{206}Pb/^{238}U$ age of 597 ± 3 Ma (MSWD = 1.18 and probability = 0.29) (Fig. A6 in the Supplementary material).

5.4 Alborán Domain

5.4.1 Paleozoic basement of the South Federico Unit of the Sebtide/Alpujárride Complex

Sample Ri119

Approximately 370 zircons with different sizes, colours, textures and morphologies were handpicked from the Ri119 zircon concentrate. From the CL images, these zircons mainly show grains with continuous oscillatory zoning and, to a lesser extent, complex grains with partially resorbed cores overgrown by high or low U rims (Fig. 5). There are also a few grains with sector zoning (Fig. 5).

One hundred and forty five zircons were analysed and 141 of 155 analyses yielded concordant or nearly concordant dates between 298 and 3189 Ma (Fig. 12 and Table A4 in the Supplementary material). The dates obtained are Paleozoic (28%), Neoproterozoic (41%), Mesoproterozoic (12%), Paleoproterozoic (14%), Neoarchean (4%) and Mesoarchean (1%) and cluster in two main populations at ca. 532 and 992 Ma (Fig. 12). The youngest zircon of sample Ri119 has a $^{206}Pb/^{238}U$ date of 298 ± 9 Ma (Table A4 in the Supplementary material) and the youngest zircon population has a

ACCEPTED MANUSCRIPT

$^{206}Pb/^{238}U$ mean age of 353 ± 6 Ma (MSWD = 1.4 and probability = 0.24) (Fig. A8 in the Supplementary material).

5.4.2 Carboniferous sandstone within the Akaili tectonic unit of the Ghomaride/Maláguide Complex.

Sample Ri121

From the zircon concentrate of this sandstone, ~ 370 zircons with different morphologies, sizes, colours and textures were handpicked. Zircon CL images show continuous oscillatory zoning and, less frequently, partially resorbed cores overgrown by thick low or high U rims (Fig. 5). There are also a few grains with sector zoning (Fig. 5).

One hundred and fifty five analyses were performed on 145 zircons, 144 of which yielded concordant or nearly concordant dates ranging between 303 and 2790 Ma (Fig. 12, and Table A4 in the Supplementary material). These dates are Paleozoic (33%), Neoproterozoic (40%), Mesoproterozoic (2%), Paleoproterozoic (19%) and Neoarchean (4%), and form three main populations at ca. 488, 595 and 2062 Ma (Fig. 12). The youngest zircon $^{206}Pb/^{238}U$ date is 303 ± 8 Ma (Table A4 in the Supplementary material) and the youngest zircon population (made of four dates) has a $^{206}Pb/^{238}U$ mean age of 330 ± 4 Ma (MSWD = 0.45 and probability = 0.72) (Fig. A8 in the Supplementary material).

6. Discussion

The studied samples can be grouped into several categories based on similar detrital age patterns: i) Mesozoic samples from the External Zones and the Maghrebian Flysch, ii) Cenozoic samples from the Tanger unit and the Numidian Fm, and iii)

ACCEPTED MANUSCRIPT

samples from the Internal Rif or Alborán Domain. One exception is sample Ri35 from the Ras Afraou unit that will be discussed separately.

6.1 Mesozoic samples from the External Zones and the Maghrebian Flysch

The similarity in the detrital age distribution for all Mesozoic samples is noteworthy; particularly for the ubiquitous scarcity of Mesozoic grains (see Fig. 6, 9 and 11). Only three of the samples from the Temsamane, Tanger-Ketama and 'internal' Mauretanian Tisiren Unit contain zircons younger than Paleozoic (sample BKM3: one Triassic grain at 234 ± 3 Ma; sample Ri68: one Triassic grain at 227 ± 10 Ma; sample Ri43: one Cenozoic grain at 21 ± 6 Ma, and another Triassic grain at 247 ± 8 Ma). The abundance of Paleozoic grains usually ranges between 7 and 10% in the combined age spectra, and these are essentially Cambrian in age, with scarce Permian to Ordovician dates. The presence of several Devonian grains is a common feature in most samples. Neoproterozoic grains are most abundant, representing 40 to 51% of the grains in the combined age spectra. Most of them are Ediacaran and grouped into a main population with a main peak at ca. 590-599 Ma. There are also a few Cryogenian-Tonian grains. All samples have Mesoproterozoic zircon grains (15% in the combined age spectra) with several peaks (Figs. 6, 9, and 11). The samples all contain Paleoproterozoic zircon grains (23 to 30% in the combined age spectra), with Orosirian and Rhyacian secondary populations. All samples also contain a few Neoarchean grains (2 to 5%) and in several samples there are scarce Mesoarchean, Paleoarchean, and Eoarchean grains.

The zircon age distributions in the Mesozoic samples are in agreement with those determined by Pratt et al. (2015) on two samples: sample RF3 from the same Lower Cretaceous quartzitic succession of the Tanger-Ketama unit, and sample RF4 from the Lower Cretaceous Tisiren Flysch. In both studies, the same dominant

ACCEPTED MANUSCRIPT

Ediacaran population at ca. 597 Ma was recognised. There are also two small populations at ca. 1181 and 1445 Ma (Stenian and Calymmian respectively), although the results presented here do not replicate the small Tonian-Stenian population at ca. 1000 Ma noted by these authors. Furthermore, a Paleoproterozoic population, also described by Pratt et al. (2015), has been recognised in this work, ranging from ca. 1800 to 2200 Ma with several peaks at ca. 1871, 1980 and 2114 Ma.

6.2. Potential source areas for the different zircon age populations from the Mesozoic rocks of the External Rif and the Maghrebian Flysch Complex.

This work did not yield any Jurassic or Cretaceous dates in the total population of 1443 concordant-nearly concordant grains (Fig. 13). However, zircons with those ages are present in the Middle Jurassic to Early Cretaceous alkaline magmatism from the High Atlas region (Hailwood and Mitchell, 1971; Rahimi et al., 1997; Armando, 1999; Lhachmi et al., 2001; Zayane et al., 2002; Haddoumi et al., 2010; Bensalah et al., 2013). The lack of Jurassic to Cretaceous grains indicates that the source alkaline magmatic bodies were not exposed at the surface at this time, and thus they could not provide any zircon for the Mesozoic sediments of the External Rif and the Maghrebian Flysch. This is in agreement with the restored cross sections of the High Atlas suggesting that the Cretaceous rocks were post-rift sediments and covered the sedimentary infilling and igneous bodies of the Jurassic rifting (Arboleya et al., 2004).

There are Upper Ordovician to Devonian zircon grains (ca. 360-460 Ma: (see Figs. 6, 9 and 11) probably derived from Avalonian terranes, where the rifting of Avalonia from Gondwana and later collision of Avalonian with Laurentia and Baltica was recorded (e.g. Sánchez Martínez et al., 2007, 2012). The Late Devonian grains (ca.

ACCEPTED MANUSCRIPT

380-360 Ma) can be linked to granitoids like the Rabat granitoids (Tahiri et al. 2010) that are part of the Sehoul Block, an Avalonian terrane thrusting over the Moroccan Mesetas (Simancas et al., 2005; Tahiri et al., 2010) (Fig. 13). They are also present within several samples from the Paleozoic Moroccan Mesetas (Accotto et al., 2018). In addition, zircons with similar dates in the SW Iberian Massif are attributed to a cryptic Rheic volcanic arc in Iberia (Pereira et al., 2012; Pérez-Cáceres et al., 2017), that could be hidden below the thrust surface of the Avalonian terranes (i.e. the Sehoul Block) at present. Pratt et al. (2015) studied the Middle Jurassic Bou Rached sandstones in the Middle Atlas and found a significant population of Ordovician-Devonian zircons. They also suggested a probable origin from the Sehoul block and proposed that the zircons were stored in Carboniferous-Triassic strata in Morocco. Accotto et al. (2018) have recently confirmed this hypothesis. Data from Marzoli et al. (2017) from the Uppermost Triassic (Rhaetian, ca. 202 Ma) series of Central High Atlas and Argana basins also agree with the previous interpretation, as they found that samples interlayered with the Lower CAMP basalts contained Upper Paleozoic grains.

The Cambrian to Middle Ordovician zircon grains (ca. 540-460) (Figs. 6, 9 and 11) can be related to the magmatic events developed in the northern margin of Gondwana and associated to the opening of the Rheic Ocean that are represented in widespread magmatic bodies in the Iberian Peninsula (e. g. Talavera et al.; 2013), although there are scarce equivalents in the Variscan Moroccan Mesetas (see Letsch et al., 2018). However, there are sources of Cambrian zircons farther south, in the Lower Cambrian magmatic rocks (e.g. the Jbel Boho rocks in the Anti-Atlas, Benaouda, 2015), or in the Derraman Peralkaline Felsic Complex within the Mauritanides (see Bea et al., 2016) (Fig. 13).

ACCEPTED MANUSCRIPT

A dominant Ediacaran zircon population, with a main peak ca. 590 Ma, represents the Cadomian and Pan-African orogenic events and characterizes the Neoproterozoic zircon group (40 to 51 % in the combined age spectra). This dominant Pan-African population is present in the rocks of the Sehoul Block, Bou Regreg Corridor (Tahiri et al., 2010), and both Variscan Moroccan Mesetas (Ouabid et al., 2017; Accotto et al., 2018; Letsch et al., 2018) (Fig. 13). It is also present in the northern components of the West African Craton: Anti-Atlas, Ediacaran sedimentary cover of the Reguibat Shield, Mauritanides, and the western margin of the Taoudeni Basin (see Gärtner et al., 2017 and references therein) (Fig. 13). This population is also dominant in the Triassic sediments from the Central High Atlas and Argana basins (Marzoli et al. 2017). Therefore, the sources for this Ediacaran zircon population most probably were the Variscan Mesetas and the NW African Craton (Fig. 13).

Zircon grains with ages between 750 and 900 Ma are scarce (28 grains), in contrast to the 52 zircon grains with Tonian-Late Stenian ages(ca. 900-1050 Ma). A similar distribution of Neoproterozoic-Stenian zircon grains is also observed in the Triassic rocks of the Central High Atlas basin (Marzoli et al. 2017), and in the Paleozoic rocks from the Moroccan Mesetas, where the Tonian-Late Stenian zircons can reach even 24-31% of the total sample (Accotto et al., 2018). The Tonian grains are also present in the Paleozoic sediments from the Central Iberian, West Astur-Leonian and Cantabrian zones of the Iberian Massif (Bea et al., 2010; Díez Fernández et al., 2010; Cambeses, 2015, among others). This Tonian population is usually related to the Grenville orogeny and can be sourced from Avalonian, Baltic, or Amazonian terranes. Alternatively, Bea et al. (2010) proposed that these grains were derived from the Saharan metacraton and, most probably, from the Arabian-Nubian shield, and incorporated to the sediments of the northern Gondwana terranes. We propose a similar

ACCEPTED MANUSCRIPT

origin for the Tonian-Late Estenian grains, which were incorporated within the Paleozoic rocks of the Variscan Moroccan Mesetas (see Accotto et al., 2018), later eroded, and deposited in the Riffian paleomargin.

In NW Africa, there is a distinctive and characteristic gap of zircon ages between 1.1 and 1.6 Ga (see Gärtner et al., 2017, and references therein, but also Letsch et al., 2018) (Fig. 13). However, 15% of all the ages in the combined age spectra from this work are of this age, to the extent that there are secondary Stenian (Ri43, 1181 Ma), Ectasian (Ri102, ca. 1213 Ma) and Calymmian populations in several samples (Fig. 13). The nearest sources with Neoproterozoic sediments with significant Mesoproterozoic zircon populations have been studied by Gärtner et al. (2017) and include part of the cover of the Reguibat shield, the Mauritanides, and the western margin of the Taoudeni Basin (Fig. 13). Therefore, in order to explain these secondary populations, the zircons must have been transported from the Reguibat massif and other central components of the West African Craton, towards the Mesozoic African paleomargin (Fig. 13).

The proportion of Paleoproterozoic zircon grains (23 to 30% in the combined age spectra) is higher than the proportion of Mesoproterozoic grains, with the previously mentioned Orosirian and Rhyacian secondary populations representing the Eburnian-Birimian orogenic cycles (1.78-2.35 Ga, see Abati et al., 2010, and references therein). This population can be found in the Middle Jurassic of the Middle Atlas and in the Cretaceous sediments of the Riffian paleomargin (Pratt et al., 2015), but also in all the components of the West African Craton and, the Anti-Atlas, the Sehoul Block and Bou Regreg Corridor (Gärtner et al., 2017), and within the basement of the Moroccan Mesetas (Pereira et al. 2015) (Fig. 13). We can therefore interpret this population as having been sourced from one of these regions (Fig. 13).

ACCEPTED MANUSCRIPT

6.3 Ras Afraou unit sample Ri35

The Ras Afraou unit is commonly attributed a Paleozoic age, but the dates obtained here on sample Ri-35 (from the black schists and quartzites of the upper Ras Afraou unit) not only yielded a zircon population distribution that starkly contrasts all other analysed samples, but one that also calls the Paleozoic age into question (see Figs. 4, and 8). The youngest zircon population in the Ras Afraou sample is Mesozoic in age, (243 ± 3 Ma; MSWD = 1.02 and probability = 0.41) (Middle Triassic, Anisian) (Fig. A3 in the Supplementary material), and the youngest $^{206}Pb/^{238}U$ zircon date of this quartzite is 200 ± 7 Ma (Uppermost Triassic). These data discount the idea that the Ras Afraou black schists and quartzites are Paleozoic in age. Therefore, we propose a Mesozoic or younger age for these rocks, and possibly a Cretaceous age by correlation with the Albian-Lower Aptian black facies from the rest of the Temsamane and Tanger-Ketama units.

Another noticeable difference between this sample and others studied is the presence of two populations in sample Ri35 at ca. 270 Ma (Upper-Middle Permian) and ca. 320 Ma (Lower Carboniferous) that are absent in the Mesozoic Riffian samples (Figs. 6, 7, and 8). Furthermore, Ri35 has an Ediacaran zircon population (ca. 583 Ma) but it is not the dominant population as is the case in the previously described samples (see Figs. 6, 7, and 8). In addition, the Mesoproterozoic grains (2%) are nearly absent in Ri35, in contrast with the Mesozoic Riffian samples, where 15% of the grains are this age (see Figs. 6, 7, and 8).

The significantly different zircon age population distribution pattern for the Ras Afraou black schists could indicate the presence of a local source. We interpret this local source in terms of the geometry of the Riffian paleomargin, where the Temsamane domain had a proximal location (see Azdimousa et al., 2007; Jabaloy et al., 2015), the

ACCEPTED MANUSCRIPT

thick successions of the Tanger-Ketama domain were in a more distal location (see Chalouan et al., 2008; Vázquez et al., 2013), and the Ras Afraou domain was located in the transition between both. Vázquez et al. (2013) proposed the existence of a major normal fault in this transitional domain. The erosion of Paleozoic successions in the fault scarp could provide the local detritus source and explain the abundance of Paleozoic zircon grains over the Ediacaran grains in sample Ri35.

6.4 Cenozoic samples from the External Rif and the Maghrebian Flysch

Sample Ri63 from the Middle Eocene to Middle Miocene sandstones of the Tanger unit yielded 46 concordant dates ranging from 413 to 2590 Ma (Fig. 10, and Table A2 in the Supplementary material), with three main populations at ca. 627, 1041 and 1945 Ma (Fig. 10). This age distribution contrasts with that of the Mesozoic rocks from the same unit by the presence of a well-defined Tonian-Stenian population at ca. 1041 Ma.

Sample Ri64, from the Latest Oligocene to Aquitanian quartz arenite from the Numidian Fm, yielded 140 concordant analyses (Fig. 10, and Table A3 in the Supplementary material), ranging from 347 Ma to 2888 Ma. The age distributions are Paleozoic (5%), Neoproterozoic (49%), Mesoproterozoic (9%), Paleoproterozoic (31%), Neoarchean (5%) and Mesoarchean (1%), and cluster in five main populations at ca. 597, 656, 1744, 1893 and 2054 Ma (Fig. 10).

The clastic supply for the Numidian Fm is now nearly unanimously interpreted as being of African provenance (see Fornelli et al. 2015). Nevertheless, this southern provenance has traditionally been controversial and northern (European) provenance has also been proposed (Parize et al., 1986; Yaich et al., 2000; Boukhalfa et al., 2009; Riahi et al., 2010; Fildes et al., 2010), although this too has been contested (Thomas et

ACCEPTED MANUSCRIPT

al., 2010a, 2010b; Guerrera et al., 2012; Alcalá et al., 2013, Fornelli et al., 2015). The age distribution obtained in this work for the Numidian Fm is similar to that obtained on the Tanger unit, suggesting that both Cenozoic turbiditic successions had the same source areas in NW Africa, the Tanger unit probably being in a more proximal setting than the Numidian Fm. Moreover, the U-Pb zircon data (Fig. 10) are similar to populations described by Fornelli et al. (2015) on two samples from the Numidian Fm in the south Apennines (56 concordant ages), but with a Langhian depositional age.

6.5 Alborán Domain

Two samples from the Internal Rif or Alborán Domain (Ri119 from the Sebtide/Alpujárride and Ri121 from Ghomaride/ Maláguide), provide different age distribution patterns (see Fig. 12). Sample Ri119 yielded two main populations at ca. 532 and 992 Ma while Ri121 showed three main populations at ca. 487, 595 and 2062 Ma, lacking the Tonian-Stenian peak at around 1000 Ma (Fig. 12). However, both samples have common features that differentiate them from samples related to the NW African paleomargin (Fig. 12), primarily the scarcity of Mesoproterozoic zircons. In addition, there is a secondary Variscan population near 340 Ma, and another population of Neoarchaean zircons at ca. 2600 Ma. These samples also contain the youngest zircon population which points to a Carboniferous maximum depositional age (353 ± 6 Ma for Ri 119 and 330 ± 4 Ma for Ri121) (Fig. 12). Furthermore, the age distribution patterns for these two samples (Fig. 12) are different to those from the External Rif and Maghrebian Flysch Complex (Fig. 10), suggesting that the Alborán Domain was not the source area of the sediments for both paleogeographic domains, or the so-called Mauretanian Flysch.

ACCEPTED MANUSCRIPT

6.6 Paleogeographic and tectonic implications

The studied Jurassic-Cretaceous samples have a very similar U-Pb detrital zircon age distributions, with the exception of Ri35 from the Ras Afraou unit. These patterns are also similar to those of samples from the Rif Belt studied by Pratt et al (2015). Furthermore, they have a different age pattern to those of the Alborán Domain (Figs. 12 and 13), suggesting a common location in the NW African paleomargin for all these samples, including the Tisiren unit.

The U-Pb detrital zircon age distribution from this work raises a major question regarding the traditional paleogeographic interpretation of the Mauretanian Flysch, commonly interpreted to have been located in the slope-basinal paleomargin of the Alborán Domain at the conjugate margin of the Ligurian-Maghrebian Neotethys (e.g. Chalouan et al., 2008; Guerrera et al. 2012). The presence of NW African zircons within these Mesozoic sediments and contrasting zircon age population patterns relative to the Alborán Domain does not support this interpretation. The U-Pb detrital data can only be explained if the Tisiren succession was in the African Paleomargin during the Lower Cretaceous, as proposed recently by Pratt et al. (2015), forming part of the same turbiditic fan systems that sourced the Massylian Flysch.

The composite U-Pb detrital zircon age data for all Jurassic-Cretaceous samples, including samples RF3 and RF4 from Pratt et al. (2015) shows a dominant population at ca. 600 Ma, originating during the Pan-African orogeny and sourced in the Northern part of the West African Craton and the Sehoul block as previously discussed (see Fig. 13). It also includes secondary populations of Mesoproterozoic zircons at ca. 1000, 1200 and 1500 Ma that can only have been sourced from the Reguibat and other central components of the West African Craton (see Gärtner et al., 2017). In order to transport these Mesoproterozoic grains to the Neotethyan paleomargin of the Rif, the existence of

ACCEPTED MANUSCRIPT

northward-directed fluvial systems, parallel to the Central Atlantic continental margin of NW Africa, are required (Fig. 13). Low-temperature thermochronological studies on the Central Atlantic margin through the Western Moroccan Meseta, High-Atlas, Anti-Atlas and Reguibat shield, but also in the East America conjugate margin, demonstrate the existence of km-scale vertical movements during Jurassic-Early Cretaceous times (see Gouiza et al., 2018, and references therein). Subsidence movements were related to deposition of Mesozoic sediments that were later eroded during the subsequent uplift events (Gouiza et al. 2018). Davison (20055), Gouiza (2011) and Gouiza et al. (2018) propose that the eroded sediments were probably routed to the Atlantic margin, but results from this study strongly suggest that fluvial systems routed at least part of the sediments to the Riffian paleomargin. They are probably now preserved in the fluvial Cretaceous deposits of the Hamadas that cover part of the West African Craton (Zouhri et al., 2008, their Figure 7.3).

7. Conclusions

Detrital zircons from 17 samples from the External Rif, the Maghrebian Flysch Complex and the Internal Rif or Alborán Domain were studied in this work. The data include 12 samples with 1443 concordant and nearly concordant dates from Mesozoic rocks of the External Rif and the Maghrebian Flysch Complex (including the so-called Mauretanian internal flysch units) that have similar U-Pb detrital zircon age distributions. These patterns indicate that all the domains of the External Rif and the entire Maghrebian Flysch Complex were part of the same NW African paleomargin. Sample Ri35 from the so-called Paleozoic from the Ras Afraou unit, has a very different age spectra that we interpret as indicating a local source, and that includes one youngest Mesozoic zircon population (243 ± 3 Ma; MSWD = 1.02 and probability = 0.41)

ACCEPTED MANUSCRIPT

indicating a Mesozoic or younger age for these Ras Afraou rocks. We propose a likely Cretaceous age for these rocks using correlation to the Albian-Lower Aptian black facies from the rest of the successions of the External Rif.

In all the samples, there are Paleozoic (scarce ones), Neoproterozoic (with a dominant Ediacaran zircon population with a main peak ca. 590 Ma), and Paleoproterozoic zircon grains (23 to 30% in the combined age spectra) that were likely sourced from the Variscan Moroccan Mesetas, northern components of the West African Craton, or from Triassic sediments from the Central High Atlas and Argana basins. However, there are also Mesoproterozoic zircon ages between 1.1 and 1.6 Ga (15 % in the combined age spectra) for which the nearest sources was in the central part of the West African Craton (Reguibat shield, the Mauritanides, and the western margin of the Taoudeni Basin). Transport of the Mesoproterozoic grains to the NW African paleomargin required northward-directed fluvial systems parallel to the Central Atlantic continental margin of Africa.

Two Cenozoic samples from the External Rif and the Maghrebian Flysch show similar age patterns to those of the Mesozoic samples, while two samples from the Internal Rif or Alborán Domain are different to those related to the NW African paleomargin, especially in the scarcity of Mesoproterozoic zircons. This suggests that the Alborán Domain did not form part of the source areas for both the External Rif and the Maghrebian Flysch Complex.

Acknowledgements

Zircon analyses were carried out at the John de Laeter Centre, Curtin University, with the financial support of the MINECO/FEDER, Spain (CGL2015-71692-P), Australian Research Council (LE150100013) and AuScope NCRIS (AQ44

ACCEPTED MANUSCRIPT

Australian Education Investment Fund program), and the technical support of B. McDonald.

Data Availability

Datasets related to this article can be found at http://dx.doi.org/10.17632/b7wgj3pns2.1, an open-source online data repository hosted at Mendeley Data (Azdimousa, A.; Jabaloy, A.; Talavera, C.; Asebriy, L.; González-Lodeiro, F.; Evans, N. J., 2018).

References

Abati, J., Aghzer, A.M., Gerdes, A., Ennih, N., 2010. Detrital zircon ages of Neoproterozoic sequences of the Moroccan Anti Atlas belt. Precambrian Research 181, 115-128.

Accotto, C., Martínez Poyatos, D., Azor, A., Jabaloy, A., Azdimousa, A., Tahiri, A., El Hadi, H., 2018. First U/Pb detrital zircon age populations from the Eastern Variscan Moroccan Meseta. Geophysical Research Abstracts, 20, EGU2018-14857.

Alcalá, F.J., Guerrera, F., Martín-Martín, M., Raffaelli, G., Serrano, F., 2013. Geodynamic implications derived from Numidian-like turbidites deposited along the Internal-External Domain Boundary of the Betic Cordillera (Spain). Terra Nova 25, 119-129.

Andrieux, J., Fontboté, J., Mattauer, M., 1971. Sur un modèle explicatif de l'Arc de Gibraltar. Earth and Planetary Science Letters 12,191-198.

ACCEPTED MANUSCRIPT

Andrieux, J., 1971. La structure du Rif central. Notes et Mémoires de Sérvice Géologique Marocain 235, 155 p.

Arboleya, M.L., Teixell, A., Charroud, M., Julivert, M., 2004. A structural transect through the High and Middle Atlas of Morocco. Journal of African Earth Sciences 39, 319-32.7

Armando, G., 1999. Intracontinental alkaline magmatism: Geology, Petrography, Mineralogy and Geochemistry of the Jbel Hayim Massif (Central High AtlasMorocco). Mémoires de Géologie de l'Université de Lausanne 31, 106p.

Asebriy, L., 1984. Etude géologique de la zone subrifaine: nouvelle interprétation paléogéographique et structurale du Rif externe; exemple du Moyen Ouerrha, Maroc. Thèse 3ème cycle, Faculté des Sciences de l'Université Mohammed V de Rabat, 187p.

Asebriy, L., Bourgois, J., De Luca, P., Butterlin, J., 1992. Importance d'une tectonique de distension pliocène dans le Rif central (Maroc): la nappe de Kétama existe-t-elle?. Journal of African Earth Sciences 15, 49-57.

Asebriy, L., de Luca, P., Bourgois, J., Chotin, P., 1987. Resédimentation d'âge sénonien dans le Rif central (Maroc): Conséquences sur les divisions paléogéographiques et structurales de la chaîne? Journal of African Earth Sciences 6, 9-17.

Asebriy, L, Azdimousa, A., Bourgois, J., 2003. Structure du Rif externe sur la transversale du Massif de Ketama. Travaux de l'Institut Scientifique, Université Mohammed V. Série Géologie et Géographique physique 21, 27-46.

ACCEPTED MANUSCRIPT

Asebriy, L., 1994. Evolution tectonique et métamorphique du Rif central (Maroc): Définition du domaine subrifain. PhD Thesis, Université Mohammed V, Rabat, 283p.

Azañón, J.M., Crespo-Blanc, A., 2000. Exhumation during a continental collision inferred from the tectonometamorphic evolution of the Alpujarride Complex in the central Betics (Alboran Domain, SE Spain). Tectonics, 19, 549–565.

Azdimousa A., Bourgois J., Poupeau G., Montigny R. 1998. Histoire thermique du massif de Ketama (Maroc): sa place en Afrique du Nord et dans les Cordillères Bétiques. Comptes Rendus de l'Académie des Sciences, série II 326, 847-853.

Azdimousa, A., Bourgois, J., Asebriy, L., Poupeau, G., Montigny, R., 2003. Histoire thermique et surrection du Rif externe et des nappes de flyschs associées (Nord Maroc). Travaux de l'Institut Scientifique, Université Mohammed V. Série Géologie et Géographique physique 21, 15-26.

Azdimousa, A., Jabaloy, A., Asebriy, L., Booth-Rea, G., Gonzalez-Lodeiro, F., Bourgois, J., 2007. Lithostratigraphy and Structure of the Temsamane Unit (Eastern External Rif, Morocco). Revista de la Sociedad Geológica de España 20, 187-200.

[dataset] Azdimousa, A., Jabaloy, A., Talavera, C., Asebriy, L., González-Lodeiro, F., Evans, N.J. (2018) Detrital zircon U–Pb ages in the Rif Belt (northern Morocco): Paleogeographic implications, (2018, Mendeley Data, v1, http://dx.doi.org/10.17632/b7wgj3pns2.1

Azdimousa, A., Jabaloy-Sánchez, A., Münch, P., Martínez-Martínez, J.M., Booth-Rea; G., Vázquez-Vílchez, M., Asebriy, L., Bourgois, J.,

ACCEPTED MANUSCRIPT

González-Lodeiro, F. (in press) Structure and exhumation of the Cap des Trois Fourches basement rocks (Eastern Rif, Morocco). Journal of African Earth Sciences

Balanyá J.C., García-Dueñas, V., 1987. Les directions structurales dans le Domaine d´Alboran de part et d'autre du Detroit de Gibraltar, Comptes Rendus de l'Académie des Sciences, série II 304, 929-933.

Bea, F., Montero, P., Haissen, F., Molina, J.F., Michard, A., Lazaro, C., Mouttaqi, A., Errami, A., Sadki, O., 2016. First evidence for Cambrian rift-related magmatism in the West African Craton margin: The Derraman Peralkaline Felsic Complex. Gondwana Research 36. 423-438.

Bea, F., Montero, P., Talavera, C., Abu Anbar, M., Scarrow, J.H., Molina, J.F., Moreno, J.A., 2010. The paleogeographic position of Central Iberia in Gondwana during the Ordovician: evidence from zircon chronology and Nd isotopes. Terra Nova 22, 341-346.

Ben Yaich, A., 1991. Evolution tectono-sédimentaire du Rif externe centro-occidental (Régions de Msila et Ouezzane, Maroc). La marge africaine du Jurassique au Crétacé inférieur. Les bassins néogènes d'avant-fosse. PhD Thesis, University of Pau, France, 308 p.

Benaouda, R., 2015. Magmatic evolution and REE mineralization in the early Cambrian Jbel Boho igneous complex in the Bou Azzer inlier (Anti-Atlas/Morocco). PhD Thesis, Christian-Albrechts-Universität, Kiel, XXI, 140 pp.

Bensalah, M.K., Youbi, N., Mata, J., Madeira, J., Martins, L., El Hachimi, H., Bertrand, H., Marzoli, A., Bellieni, G., Doblas, M., Font, E.,

ACCEPTED MANUSCRIPT

Medina, F., Mahmoudi, A., Berraâouz, E.H., Miranda, R., Verati, C., De Min, A., Ben Abbou, M., Zayane, R., 2013. The Jurassic Cretaceous basaltic magmatism of the Oued El-Abid syncline (High Atlas, Morocco): physical volcanology, geochemistry and geodynamic implications. Journal of African Earth Sciences 81, 60-81.

Booth-Rea, G., Ranero, C.R., Martinez-Martinez, J.M., Grevemeyer, I., 2007. Crustal types and Tertiary tectonic evolution of the Albora´ n sea, western Mediterranean. Geochemistry, Geophysics Geosystems 8 (10) 13th October 2007 Q10005, doi:10.1029/2007GC001639

Bouillin, J.P., 1984. Nouvelle interprétation de la liaison Apennin-Maghrebides en Calabre; conséquences sur la paléogéographie téthysienne entre Gibraltar et les Alpes. Revue de Géographie Physique et Géologie Dynamique 25(5), 321-338.

Bouillin, J.P., Durand Delga, M., Gélard, J.P., Leikine, M., Raoult, J.F., Raymond, D., Tefiani, M., Vila, J.M., 1970. Définition d'un Flysch massylien et d'un Flysch maurétanien au sein des Flyschs allochtones de l'Algérie. Comptes Rendus de l'Académie des Sciences, série II 270, 2249-2252.

Boukhalfa, K., Ben Ismail-Lattrache, K., Riahi, S., Soussi, M., Khomsi, S., 2009. Analyse biostratigraphique et sédimentologique des séries éo-oligocènes et miocènes de la Tunisie septentrionale : implications stratigraphiques et géodynamiques. Comptes Rendus Géoscience 341, 49-62. Doi: 10.1016/j.crte.2008.10.001

Bourgois, J., 1977. D'une étape géodynamique majeure dans la genèse de l´arc de Gibraltar: "L´hispanisation des flyschs rifains au Miocène inférieur". Bulletin de la Société Géologique de la France 19, 1115-1119.

ACCEPTED MANUSCRIPT

Cambeses, A., 2015. Ossa-Morena Zone Variscan "calc-alkaline" hybrid rocks: interaction of mantle-and crustal-derived magmas as a result of intra-orogenic extension-related intraplanting. PhD Thesis, Universidad de Granada. http://hdl.handle.net/10481/40693

Chalouan, A., Michard, A., El Kadiri, K., Negro, F., Frizon de Lamotte, D., Soto J.I., Saddiqi, O., 2008. The Rif Belt. In: Michard, A., Frizon de Lamotte, D., Saddiqi, O., Chalouan, A., (Eds.) Continental Evolution: The Geology of Morocco. Lecture Notes in Earth Sciences, vol 116, pp. 203-302, Springer-Verlag, Berlin Heidelberg.

Ciszak, R., 1987. Resédimentation intra-sénonienne du Trias évaporitique dans le sillon tellien (Algérie). Implications dans la tectogenèse des Maghrébides. Géologie Mediterranéenne 14, 137-141.

Ciszak, R., Magne, J., Peybernes, B., 1986. Interprétation du complexe chaotique "triasique" d'Oranie (Algérie occidentale) comme un olistostrome sénonien localement réinjecté dans les accidents alpins. Comptes Rendus de l'Académie des Sciences, série II 402, 357-362.

Davison, I., 2005. Central Atlantic margin basins of North West Africa: Geology and hydrocarbon potential (Morocco to Guinea). Journal of African Earth Sciences 43, 254-274, doi:10.1016/j.jafrearsci.2005.07.018

Dewey, J.F., Helman, M.L., Turco, E., Hutton, D.H.W., Knott, S.D., 1989. Kinematics of the Western Mediterranean. Geological Society of London Special publication 45, pp. 265-283.

ACCEPTED MANUSCRIPT

Didon, J., Hoyez, B., 1978. Les séries à faciès mixtes, numidien et gréso-micacé, dans le Rif occidental (Maroc). Compte rendu sommaire des séances de la Société géologique de France 6, 304-307.

Díez Fernández, R., Martínez Catalán, J.R.M., Gerdes, A., Abati, J., Arenas, R., Fernández-Suárez, J., 2010. U–Pb ages of detrital zircons from the Basal allochthonous units of NW Iberia: Provenance and paleoposition on the northern margin of Gondwana during the Neoproterozoic and Paleozoic. Gondwana Research 18, 385–399.

Durand-Delga, M., Hottinger, L., Marcais, J., Milliard, Y., Suter, G., 1962. Données actuelles sur la structure du Rif. Société Géologique de France, Mémoires hors de série 1, 399-422.

Durand-Delga, M., Gardin, S., Olivier, Ph., 1999. Datation des Flyschs éocrétacés maurétaniens des Maghrébides: la formation du Jbel Tisirène, Comptes Rendus de l'Académie des Sciences, série II 328, 701-709.

Durand-Delga, M., 2006. Geological adventures and misadventures of the Gibraltar Arc, Zeitschrift für Geologische Wissenschaften 157, 687-716.

Duran-Delga, M., Rossi, P., Olivier, P., Puglisi, D., 2000, Situation structurale et nature ophiolitique de roches basiques jurassiques associées aux flyschs maghrébins du Rif (Maroc) et de Sicile (Italie), Comptes Rendus de l'Académie des Sciences de Paris, Series II 331, 29-38.

Esteras, M., Martín-Algarra, A., Martín-Martín, M., 2004. Estratigrafía. In: Vera JA (ed). Geología de España, pp. 391-395, SGE-IGME, Madrid.

Faccenna, C., Piromallo, C., Crespo-Blanc, A., Jolivet, L., Rossetti, F., 2004. Lateral slab deformation and the origin of the western Mediterranean arcs. Tectonics 23: doi: 10.1029/2002TC001488.

ACCEPTED MANUSCRIPT

Favre, P., 1992. Géologie des massifs calcaires situés au front Sud de l'unité de Kétama (Rif, Maroc). PhD Thesis. University of Genève.

Feinberg, H., 1978-1986. Les séries tertiaires du Prérif et des dépendances post-tectoniques du Rif (Maroc). PhD Thesis, University of Toulouse. Notes et Mémoires du Service Géologique Marocain, 315, 192 pp., Rabat, Maroc.

Filde,s C., Stow, D., Riah,i S., Soussi, M., Patel, U., 2010. European provenance of the Numidian Flysch in northern Tunisia. Terra Nova 22, 94-102. doi: 10.1111/j.1365-3121.2009.00921.x

Fornelli, A., Micheletti, F., Langone, A., Perrone, V., 2015. First U-Pb detrital Zircon ages from Numidian Sandstones in Southern Apennines (Italy): Evidences of Numidian provenance. Sedimentary Geology 320,19-29.

Frizon de Lamotte, D., 1985. La structure du Rif oriental (Maroc). Rôle de la tectonique longitudinale et importance des fluides. PhD Thesis. University Pierre et Marie Curie, Paris VI, Mémoires des Sciences de la Terre de la Université Pierre et Marie Curie 85-03, Paris, France.

Frizon de Lamotte, D., 1987b. La structure du Rif externe (Maroc): Mise au point sur le rôle des décrochements des chevauchements et des glissements gravitaires. Journal of African Earth Sciences 6, 755-766.

Frizon de Lamotte, D., 1987a. Un exemple de collage synmétamorphe: la déformation miocène des Temsamane (Rif, Maroc). Bulletin de la Société Géologique de France 3, 337-344.

Gärtner, A., Youbi, N., Villeneuve M., Sagawe A., Hofmann M., Mahmoudi A., Boumehdi, M.A., Linnemann U., 2017. The zircon evidence of

ACCEPTED MANUSCRIPT

temporally changing sediment transport-the NW Gondwana margin during Cambrian to Devonian time (Aoucert and Smara areas, Moroccan Sahara). International Journal of Earth Sciences 106(8), 2747-2769.

Gouiza, M., 2011. Mesozoic Source-to-Sink Systems in NW Africa: Geology of Vertical Movements During the Birth and Growth of the Moroccan Rifted Margin. Ph.D Thesis, Vrije Universiteit Amsterdam,The Netherlands.

Gouiza, M., Bertotti, G., Andriessen, P.A.M., 2018. Mesozoic and Cenozoic thermal history of the Western Reguibat Shield (West African Craton). Terra Nova 30, 135-145.

Guerrera, F., Martín-Algarra, A., Martín-Martín, M., 2012. Tectono-sedimentary evolution of the "Numidian Formation" and Lateral Facies (southern branch of the western Tethys: constraints for central-western Mediterranean geodynamics. Terra Nova 24, 3-41.

Guerrera F, Puglisi D (1984) Le Arenarie di Yesomma in Somalia: un possibile equivalente meridionale delle piu' note ''Nubian Sandstones''. Rendiconti della Società Geologica Italiana 6, 43-47.

Guerrera, F., 1981-1982. Successions turbiditiques dans les flyschs maurétanien et numidien. Revue de Géologie Dynamique et de Géographie Physique 23, 465-580.

Guerrera, F., Martin-Algarra, A., Perrone, V., 1993. Late Oligocene-Miocene syn-late-orogenic successions in Western and Central Mediterranean Chains from the Betic Cordillera to the Southern Apennines. Terra Nova 5, 525-544

ACCEPTED MANUSCRIPT

Guerrera, F., Martín-Martín, M., 2014. Geodynamic events reconstructed in the Betic, Maghrebian, and Apennine chains (central-western Tethys). Bulletin de la Société Géologique de France 185, 329-341.

Haddoumi, H., Charrière, A., Mojon, P.O., 2010. Stratigraphie et sédimentologie des «Couches rouges» continentales du Jurassique-Crétacé du Haut Atlas central (Maroc): implications paléogéographiques et géodynamiques. Geobios 43, 433–451.

Hailwood, E.A., Mitchell, J.G., 1971. Paleomagnetic and radiometric dating results from Jurassic intrusions in South Morocco. Geophysical Journal of the Royal Astronomical Society 41, 213-236.

Hoyez B., 1989. Le Numidien et les flyschs oligo-miocènes de la bordure sud de la Méditerranée occidentale, PhD Thesis, University of Lille, 464 pp.

Jabaloy-Sánchez, A., Azdimousa, A., Booth-Rea, G., Asebriy, L., Vázquez-Vílchez, M., Martínez-Martínez, J.M., Gabites, J., 2015. The structure of the Temsamane fold-and-thrust stack (eastern Rif, Morocco): Evolution of a transpressional orogenic wedge. Tectonophysics 663, 150–176.

Jackson, S.E., Pearson, N.J., Griffin, W.L., Belousova, E.A., 2004. The application of laser ablation-inductively coupled plasma-mass spectrometry to in situ U–Pb zircon geochronology. Chemical Geology 211, 47-69.

Sláma, J., Košler, J., Condon, D.J., Crowley, J.L., Gerdes, A., Hanchar, J.M., Horstwood, M.S.A., Morris, G.A., Nasdala, L., Norberg, N., Schaltegger, U., Schoene. B., Tubrett, M.N., Whitehouse, M.J., 2008. Plešovice zircon - A new natural reference material for U–Pb and Hf isotopic microanalysis. Chemical Geology 249, 1-35.

ACCEPTED MANUSCRIPT

Jolivet, L., Faccenna, C., Goffé, B., Burov, E., Agard, A., 2003. Subduction tectonics and exhumation of high-pressure metamorphic rocks in the Mediterranean orogens. American Journal of Science 303, 353-409.

Kerzazi K., 1994. Etudes biostratigraphique du Miocène sur la base des foraminifères planctoniques et nannofossiles calcaires dans le Prérif et la marge atlantique du Maroc (site 547A du DSDP Leg 79); aperçu sur leur paléoenvironnement. PhD Thesis, University Pierre et Marie Curie, Paris, 230 pp.

Kuhnt, W., Obert, D., 1991. Evolution crétacée de la marge tellienne. Bulletin de la Société Géologique de France 162, 515-522.

Leblanc, D., 1975-1979. Etude géologique du Rif externe oriental au Nord de Taza (Maroc). PhD Thesis, University Paul Sabatier, Toulouse, Notes et Mémoires du Service Géologique Du Maroc 281, 160 pp.

Lespinasse, P., 1975. Géologie des zones externes et des flyschs entre Chaouen et Zoumi (Centre de la chaîne rifaine, Maroc). PhD Thesis, University ofParis VI, 248 pp.

Letsch, D., El Houicha, M., von Quadt, A., Winkler, W., 2018. A missing link in the peri-Gondwanan terrane collage: the Precambrian basement of the Moroccan Meseta and its lower Paleozoic cover. Canadian Journal of Earth Sciences 55, 33-51. Doi: dx.doi.org/10.1139/cjes-2017-0086

Levy, R.G., Tilloy, R., 1952. Maroc septentrional (chaîne du Rif). Partie B, livret guide des excursions A31.C31. In : Congrès Géologique International, XIX session- Alger, série : Maroc, pp 8-65.

Lhachmi, A., Lorand, J.P., Fabries, J., 2001. Pétrologie de l'intrusion alcaline mésozoïque de la région d'Anemzi, Haut Atlas Central, Maroc. Journal of African Earth Sciences 32, 741-764.

ACCEPTED MANUSCRIPT

Martín-Algarra, A., 1987. Evolución geológica alpina del contacto entre las Zonas internas y las Zonas externas de la Cordillera Bética. PhD Thesis, University of Granada, 1171 pp.

Marzoli, A., Davies, J., Youbi, N., Merle, R., Dal Corso, J., Dunkley, D., Fioretti, A.M., Bellieni, G., Medina, F., Wotzlaw, J.-F., McHone, G., Font, E., Bensalah, M., 2017. Proterozoic to Mesozoic evolution of North-West Africa and Peri-Gondwana microplates: Detrital zircon ages from Morocco and Canada: Lithos 278-281, 229-239.

Michard, A., Negro. F., Saddiqi, O., Bouybaouene, M.L., Chalouan, A., Montigny, R., Goffé, B., 2006. Pressure-temperature-time constraints on the Maghrebide mountain building: evidence from the Rif-Betic transect (Morocco, Spain), Algerian correlations, and geodynamic implications. Comptes Rendus Géoscience 338, 92-114.

Michard, A., Fenberg, H., El-Azzab, D., Bouybaouene, M.L., Saddiqi, O., 1992. A Serpanite ridge in a collisional paleomargin detting: the Beni Malek massif, External Rif, Morocco. Earth and Planetary Sciences Letters 113, 435-442.

Michard, A., 1976. Elements de Géologie Marocaine. Notes Mémoires du Service Géologique du Maroc 258, 408.

Michard, A., Chalouan, A., Saddiqi, O. 2018. Continental Evolution: The Geology of Morocco. Structure, Stratigraphy, and Tectonics of the Africa-Atlantic-Mediterranean Triple Junction. Lecture Notes in Earth Sciences 116. Springer-Verlag, Berlin.

Michard, A., Hoepffner, A., Soulaimani, A., Baidder, L. 2008. The Variscan belt. In: Michard, A., Chalouan, A., Saddiqi, O. (Eds.) Continental

ACCEPTED MANUSCRIPT

Evolution: The Geology of Morocco. Structure, Stratigraphy, and Tectonics of the Africa-Atlantic-Mediterranean Triple Junction. Lecture Notes in Earth Sciences 116, pp. 65-132. Springer-Verlag, Berlin.

Monie, P., Frizon de Lamotte, D., Leikine, M., 1984. Etude géochronologique préliminaire par la méthode $^{39}Ar/^{40}Ar$ du métamorphisme alpin dans le Rif externe (Maroc). Précisions sur le calendrier tectonique tertiaire. Revue de Géologie Dynamique et de Géographie Physique 25, 307-317.

Nasdala, L., Hofmeister, W., Norberg, N., Mattinson, J.M., Corfu, F., Dörr, W., Kamo, S.L., Kennedy, A.K., Kronz, A., Reiners, P.W., Frei, D., Košler, J., Wan, Y., Götze, J., Häger, T., Kröner, A., Valley, J.W., 2008. Zircon M257 - a homogeneous natural reference material for the ion microprobe U-Pb analysis of zircon. Geostandards and Geoanalytical Research 32, 247-265.

Negro, F., de Sigoyer, J., Goffé, B., Saddiqi, O., Villa, I.M., 2008. Tectonic evolution of the Betic–Rif arc: New constraints from $^{40}Ar/^{39}Ar$ dating on white micas in the Temsamane units (External Rif, northern Morocco). Lithos 106, 93-109.

Negro, F., 2005. Exhumation des roches métamorphiques du Domaine d'Alboran: étude de la chaîne rifaine (Maroc) et corrélation avec les Cordillères bétiques (Espagne). PhD Thesis, University of Toulouse, 229 pp.

Negro, F., Agard, P., Goffé, B., Saddiqi, O., 2007. Tectonic and metamorphic evolution of the Temsamane units, External Rif

ACCEPTED MANUSCRIPT

(northern Morocco): implications for the evolution of the Rif and the Betic-Rif arc. Journal of the Geological Society of London 164, 829-842.

Ouabid, M., Ouali, H., Garrido, C.J., Acosta-Vigil, A., Román-Alpiste, M.J., Dautria, J.M., Marchesi, C., Hidas, K., 201. Neoproterozoic granitoids in the basement of the Moroccan Central Meseta: Correlation with the Anti-Atlas at the NW paleo-margin of Gondwana. Precambrian Research 299, 34-57.

Parize, O., Beaudoin, B., Burollet, P.F., Cojan, I., Fries, G., Pinault, M., 1986. La provenance du matériel gréseux numidien est septentrionale (Sicile et Tunisie). Comptes Rendus de l'Académie des Sciences de Paris 303, 1671-1674.

Paton, C., Hellstrom, J., Paul, B., Woodhead, J., Hergt, J., 2011. Iolite: freeware for the visualisation and processing of mass spectrometric data. Journal of Analytical Atomic Spectrometry 26, 2508-2518.

Pendón, J.G., 1977. Diferentes tipos de trazas orgánicas existentes en las turbiditas del Campo de Gibraltar. Estudios geológicos 33, 23-33.

Pereira, M.F., Solá, A.R., Chichorro, M., Lopes, L., Gerdes, A., Silva, J.B., 2012. North Gondwana assembly, break up and paleogeography: U-Pb isotope evidence from detrital and igneous zircons of Ediacaran and Cambrian rocks of SW Iberia (Estremoz Anticline). Gondwana Research 22, 866-881. doi:10.1016/j.gr.2012.02.010

Pérez-Cáceres, I., Poyatos, D.M., Simancas, J.F., Azor, A. 2017.Testing the Avalonian affinity of the South Portuguese Zone and the

ACCEPTED MANUSCRIPT

Neoproterozoic evolution of SW Iberia through detrital zircon populations. Gondwana Research 42, 177-192.

Platt, J.P., Allerton, S., Kirker, A., Mandeville, C., Mayfield, A., Platzman, E.S., Rimi, A., 2003. The ultimate arc: Differential displacement, oroclinal bending, and vertical axis rotation in the External Betic-Rif arc. Tectonics 22, 1-29.

Platzman, E.S., Platt, J.P., Olivier, P., 1993. Paleomagnetic rotations and fault kinematics in the Rif Arc of Morocco. Journal of the Geological Society of London 150, 707-718.

Pratt, J.R., Barbeau, Jr. D.L., Garver, J.I., Emran, A., Izykowski, Tyler, M., 2015. Detrital Zircon Geochronology of Mesozoic Sediments in the Rif and Middle Atlas Belts of Morocco: Provenance Constraints and Refinement of the West African Signature. The Journal of Geology 123, 177-200. Doi: 10.1086/681218

Rahimi, A., Saidi, A., Bouabdelli, M., Beraâouz, E.H., Rocci, G., 1997. Cristallisation et fractionnement de la série intrusive post-liasique du massif de Tasraft (Haut-Atlas central, Maroc). Comptes Rendus de l'Académie des Sciences, Paris, Séries Iia, 324, 197-203.

Riahi, S., Soussi, M., Boukhalfa, K., Ben Ismail-Lattrache, K., Dorrik, S., Khomsi, S., Bedir, M., 2010. Stratigraphy, sedimentology and structure of the Numidian Flysch thrust belt in northern Tunisia. Journal of African Earth Sciences 57, 109-126.

Díez-Fernández, R., Martínez Catalán, J.R., Gerdes, A., Abati, J., Arenas, R., Fernández-Suárez, J., 2010. U-Pb ages of detrital zircons from the Basal allochthonous units of NW Iberia: Provenance and paleoposition

ACCEPTED MANUSCRIPT

on the northern margin of Gondwana during the Neoproterozoic and Paleozoic. Gondwana Research 18, 385-399. doi:10.1016/j.gr.2009.12.006

Sánchez-Martínez, S., Arenas, R., García, F.D., Martínez-Catalán, J.R., Gómez-Barreiro, J., Pearce, J.A., 2007. Careon ophiolite, NW Spain: suprasubduction zone setting for the youngest Rheic Ocean floor. Geology 35, 53-56.

Sánchez Martínez, S., Gerdes, A., Arenas, R., Abati, J., 2012. The Bazar Ophiolite of NW Iberia: a relic of the Iapetus-Tornquist Ocean in the Variscan suture: Terra Nova 24, 283-294.

Simancas ,J.F, Tahiri, A., Azor, A., González Lodeiro, F., Martínez Poyatos, D.J., El Hadi, H., 2005. The tectonic frame of the Variscan–Alleghanian orogen in Southern Europe and Northern Africa. Tectonophysics 398, 181-198.

Stern, R.A., Bodorkos, S., Kamo, S.L., Hickman, A.H., Corfu, F., 2009. Measurement of SIMS Instrumental Mass Fractionation of Pb Isotopes During Zircon Dating. Geostandards and Geoanalytical Research 33, 145-168.

Suter, G., 1980. Carte structurale de la chaîne rifaine à 1/500000. Notes et Mémoires du Service Géologique, Maroc.

Tahiri, A., Montero, P., El Hadi, H., Martínez Poyatos, D., Azor, A., Bea, F., Simancas, J.F., González Lodeiro, F., 2010. Geochronological data on the Rabat–Tiflet granitoids: Their bearing on the tectonics of the Moroccan Variscides. Journal of African Earth Sciences 57, 1-13.

Talavera G., Montero, P., Bea, F., González Lodeiro, F., Whitehouse, M., 2013. U-Pb Zircon geochronology of the Cambro-Ordovician metagranites and metavolcanic rocks of central and NW Iberia. International Journal of Earth Sciences 102, 1-23.

ACCEPTED MANUSCRIPT

Thomas, M.F.H., Bodin, S., Redfern, J., Irving, D.H.B., 2010. A constrained African craton source for the Cenozoic Numidian Flysch: Implications for the paleogeography of the western Mediterranean basin. Earth-Science Reviews 101, 1-23.

Vázquez, M., Asebriy, L., Azdimousa, A., Jabaloy, A., Booth-Rea, G., Barbero, L., Mellini, M., Gonzalez-Lodeiro, F., 2013. Evidence of extensional metamorphism associated to Cretaceous rifting of the North-Maghrebian passive margin: The Tanger-Ketama Unit (External Rif, northern Morocco). Geol. Acta 11, 277–293.

Vera, J.A., (Ed.) 2004. Geología de España. SGE-IGME, Madrid, Spain

Vidal, J.F., 1971. Une interprétation nouvelle des nappes du Prérif central (Maroc) et ses conséquences sur la structure de leur substratum autochtone. Comptes Rendus de l´Académie des Sciences de Paris, Séries D 272, 24-27.

Wiedenbeck, M., Allé, P., Corfu, F., Griffin, W.L., Meier, M., Oberli, F., von Quadt, A., Ruddick, J.C., Spiegel, W., 1995. Three natural zircon standards for U-Th–Pb, Lu-Hf, trace element and REE analyses. Geostandards Newsletters 19, 1-23.

Yaich, C., Hooyberghs, H.J.F., Durlet, C., Renard, M., 2000. Corrélation stratigraphique entre les unités oligo-miocènes de Tunisie centrale et le Numidien. Comptes Rendus de l'Académie des Sciences, Series IIa, Earth and Planetary Science 331, 499-506.

Zaghloul, M.N., Di Staso, A., Gigliuto, L.G., Maniscalco, R., Puglisi, D., 2005. Stratigraphy and provenance of Lower and Middle Miocene strata within the External Tanger Unit (Intra-Rif sub-Domain, External

ACCEPTED MANUSCRIPT

Domain; Rif, Morocco): first evidence. Geologica Carpathica 56, 517-530.

Zayane, R., Essaifi, A., Maury, R.C., Piqué, A., Laville, E., Bouabdelli, M., 2002. Cristallisation fractionnée et contamination crustale dans la série magmatique jurassique transitionnelle du Haut Atlas central (Maroc). Comptes Rendus Géoscience, 334, 97-104. Doi: S1631-0713(02)01716-9

Zouhri, S., Kchikach, A., Saddiqi, O., El Haïmer, F.Z., Baidder, L., Michard, A., 2008. The Cretaceous-Tertiary Plateaus. In: Michard, A., Frizon de Lamotte, D., Saddiqi, O., Chalouan, A., (Eds.) Continental Evolution: The Geology of Morocco. Lecture Notes in Earth Sciences, vol 116, pp. 331-358, Springer-Verlag, Berlin Heidelberg.

ACCEPTED MANUSCRIPT

ACCEPTED MANUSCRIPT

Figure and Table captions

Figure 1.- A) Tectonic sketch of the western Mediterranean Sea, and B) Tectonic map of the Rif Chain. Squares indicate regions expanded in Figures 2 and 3.

Figure 2.- Geological map of the eastern Rif Chain with sample locations.

Figure 3.- Geological map of the western Rif Chain with sample locations.

Figure 4.- A) Lithological columns of the studied successions in the External Domain and Maghrebian Flychs. All lithological columns have the same vertical scale. Temsamane and Ras Afraou successions are modified from Azdimousa et al. (2007). For the Tanger-Ketama successions, the Ketama unit is modified from Frizon de Lamotte (1985), while the Tanger unit is modified from Zaghloul et al. (2005). For the Maghrebian Flysch succesions: the Chouamat-Meloussa unit succession is modified from Andrieux (1971), the Tisiren unit succession is modified from Durand-Delga et al. (1999), and that of the Numidian Fm is modified from Vera 2004.

Figure 5.- Cathodoluminescence images of representative dated zircons of the samples from the Rif belt.

Figure 6.- U–Pb age probability plots of the individual samples from the Lower Cretaceous rocks of the Temsamane units. Ellipses represent 2σ uncertainties.

Figure 7.- U–Pb age probability plots of the combined samples from the Lower Cretaceous rocks of the Temsamane units. Ellipses represent 2σ uncertainties.

Figure 8.- U–Pb age probability plots of sample Ri35 from the black schists and quartzites of the upper Ras Afraou unit.

Figure 9.- U–Pb age probability plots of the individual samples from the Mesozoic rocks of the Tanger-Ketama unit. Ellipses represent 2σ uncertainties.

ACCEPTED MANUSCRIPT

Figure 10.- U–Pb age probability plots of the individual samples from the Cenozoic samples. Ellipses represent 2σ uncertainties.

Figure 11.- U–Pb age probability plots of the individual samples from the Mesozic samples from the Tisiren unit. Ellipses represent 2σ uncertainties.

Figure 12.- U–Pb age probability plots of the individual samples from the Internal Rif or Alborán Domain. Ellipses represent 2σ uncertainties.

Figure 13.- Tectonic map of north-westernmost Africa showing the northern part of the West African Craton (WAC) and the adjoining fold belts (modified from Michard et al., 2008). To the right, we have added the probability plots from the samples from the Internal Rif or Alborán Domain, the Mesozoic samples (including those from Pratt et al., 2015), and the Cenozoic samples from the External Rif and Maghrebian Flysch Complex (MPZ = Mesoproterozoic zircons). The areal distribution of sediments with significant Mesoproterozoic zircons and the available data of the zircon record from the main geological components of the West African Craton, Anti Atlas and Sehoul Block are modified from Gärtner et al. (2017)

ACCEPTED MANUSCRIPT

ACCEPTED MANUSCRIPT

Table 1

SAMPLES	UTM zone	X	Y	Unidad	Rocks	Stratigraphic Age	Tectonic unit or Complex
TEM5	30N	449558	3884713	Temsamane Units	Sandstones	Aptian-Albian	Temsamane units
TEM6	30N	451427	3883617	Temsamane Units	Sandstones	Aptian-Albian	Temsamane units
TEM7	30N	467172	3888868	Temsamane Units	Sandstones	Aptian-Albian	Temsamane units
BMK3	30S	435893	3880434	Temsamane Units	Sandstones	Aptian-Albian	Temsamane units
Ri35	30N	459349	3894139	Temsamane Units	Sandstones	Paleozoic?	Ras Afrou unit
Ri66	30N	460641	3890657	Temsamane Units	Sandstones	Aptian-Albian	Temsamane units
Ri68	30N	459972	3886465	Temsamane Units	Sandstones	Aptian-Albian	Temsamane units
Ri102	30N	381348	3842244	Tanger-Ketama Unit	Sandstones	Middle-Late Jurassic	Ketama unit
Ri107	30N	381411	3841511	Tanger-Ketama Unit	Sandstones	Middle-Late Jurassic	Ketama unit
Ri63	30N	294608	3893248	Tanger-Ketama Unit	Sandstones	Eocene	Tanger unit
Ri114	30N	350763	3858139	Tanger-Ketama Unit	Sandstones	Aptian-Albian	Ketama unit
Ri43	30N	335575	3872987	Tanger-Ketama Unit	Sandstones	Aptian-Albian	Ketama unit
Ri111	30N	369201	3871345	Maghrebian Flyschs	Sandstones	Aptian-Albian	Tisiren unit
Ri 117	30N	351128	3893248	Maghrebian Flyschs	Sandstones	Aptian-Albian	Tisiren unit
Ri 64	30N	435676	3846379	Maghrebian Flyschs	Sandstones	Aquitanian	Numidian Fm
Ri119	30N	325689	3893075	Alborán Domain	Sandstones	Carboniferous	Sebtides/Alpujárrides
Ri121	30N	327557	3889339	Alborán Domain	Sandstones	Carboniferous	Ghomarides/Maláguides

ACCEPTED MANUSCRIPT

Highlights

- Detrital zircon U-Pb age from the External Rif and Maghrebian Flysch samples are very similar
- The whole Maghrebian Flysch Complex were part of the NW African paleomargin
- The so-called Mauretanian internal flysch was not related to the Alborán domain
- Part of the zircons of the Rif belt were sourced from the central West African Craton

ACCEPTED MANUSCRIPT

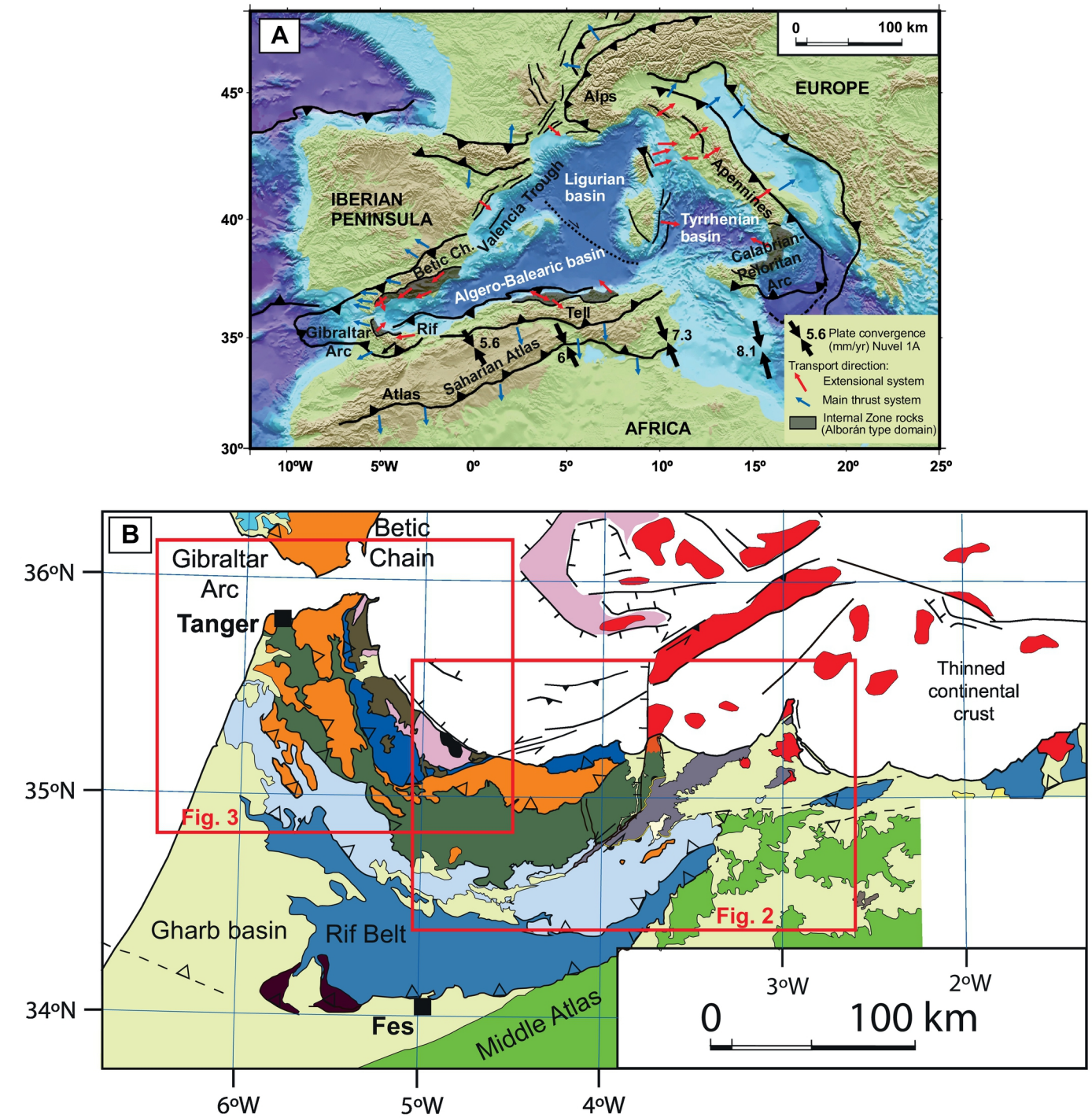
A
0
100 km
EUROPE
Alps
Ligurian basin
Apennines
IBERIAN PENINSULA
Valencia Trough
Tyrrhenian basin
Betic Ch.
Calabrian-Peloritan Arc
Algero-Balearic basin
Tell
Gibraltar Arc
Rif
5.6
7.3
8.1
6
Saharian Atlas
Atlas
AFRICA
5.6 Plate convergence (mm/yr) Nuvel 1A
Transport direction:
Extensional system
Main thrust system
Internal Zone rocks (Alborán type domain)
45°
40°
35°
30°
10°W
5°W
0°
5°
10°
15°
20°
25°
B
Betic Chain
Gibraltar Arc
Tanger
Thinned continental crust
Fig. 3
Fig. 2
Gharb basin
Rif Belt
Fes
Middle Atlas
3°W
2°W
0
100 km
36°N
35°N
34°N
6°W
5°W
4°W
Post-orogenic rocks
Late Miocene-Quaternary sediments
Neogene volcanics
Internal Rif or Alborán Domain
Frontal units ("Dorsal Calcaire")
Maláguide-Ghomaride Complex
Alpujárride-Sebtide Complex
Peridotites
South Iberian paleomargin
Middle Atlas & Moroccan Mesetas
External Rif (North African paleomargin)
"Rides pre-Rifennes"
Olistostromes of the Pre-Rif Zone
Subrif Zone
Loukos and Rifian nappes (diagenesis)
Tanger-Ketama Unit (diagenesis-anchizone)
Temsamane fold-and-thrust stack (epizone)
Maghrebian Flysch Complex
Reverse fault
High angle normal fault
Low angle normal fault

Figure 1

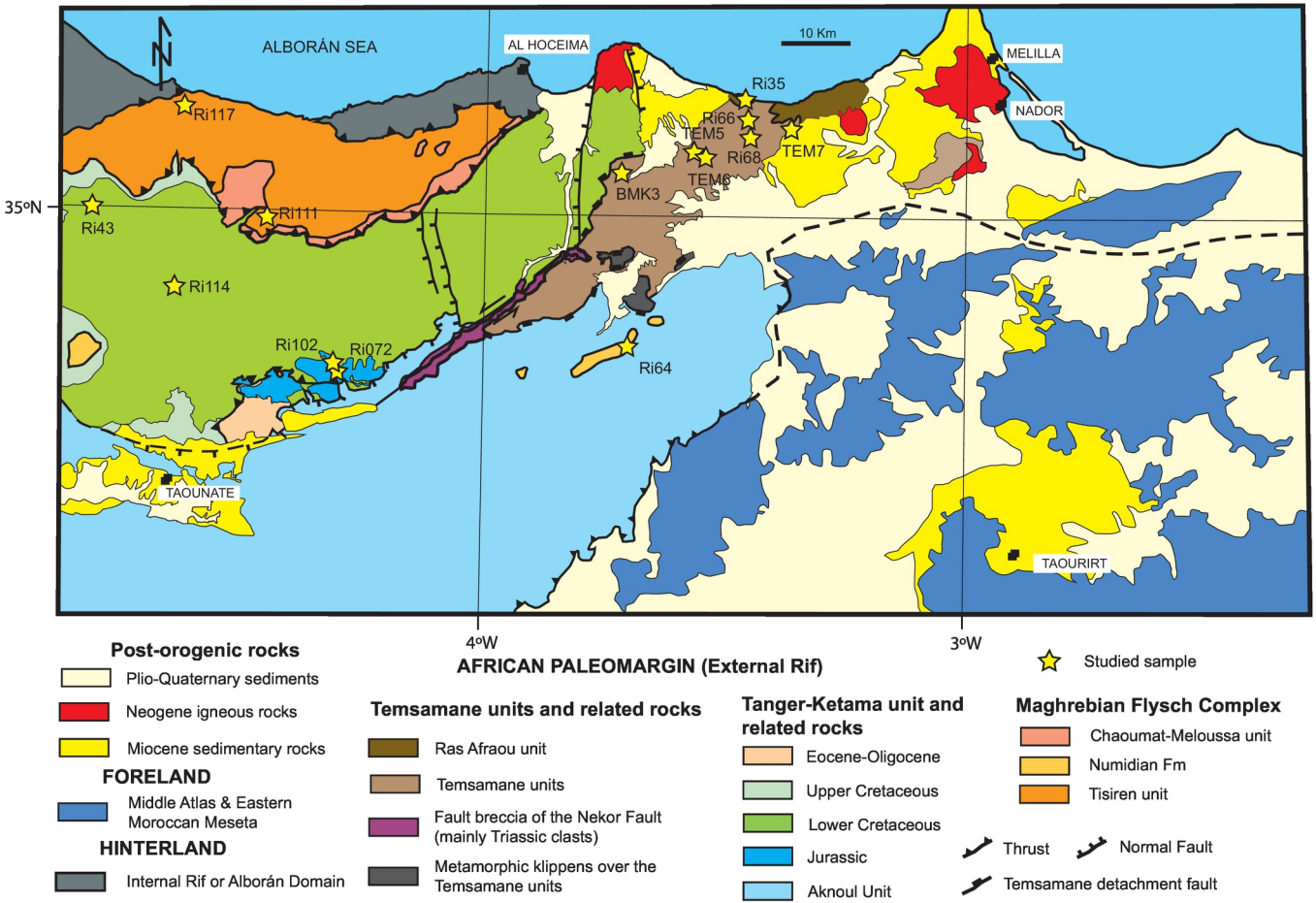
N
ALBORÁN SEA
AL HOCEIMA
10 Km
MELILLA
NADOR
Ri35
Ri66
TEM5
Ri68
TEM7
TEM6
BMK3
Ri117
Ri111
Ri43
Ri114
Ri102
Ri072
Ri64
TAOUNATE
TAOURIRT
35ºN
4ºW
3ºW
Post-orogenic rocks
Plio-Quaternary sediments
Neogene igneous rocks
Miocene sedimentary rocks
FORELAND
Middle Atlas & Eastern Moroccan Meseta
HINTERLAND
Internal Rif or Alborán Domain
AFRICAN PALEOMARGIN (External Rif)
Temsamane units and related rocks
Ras Afraou unit
Temsamane units
Fault breccia of the Nekor Fault (mainly Triassic clasts)
Metamorphic klippens over the Temsamane units
Tanger-Ketama unit and related rocks
Eocene-Oligocene
Upper Cretaceous
Lower Cretaceous
Jurassic
Aknoul Unit
Studied sample
Maghrebian Flysch Complex
Chaoumat-Meloussa unit
Numidian Fm
Tisiren unit
Thrust
Normal Fault
Temsamane detachment fault

Figure 2

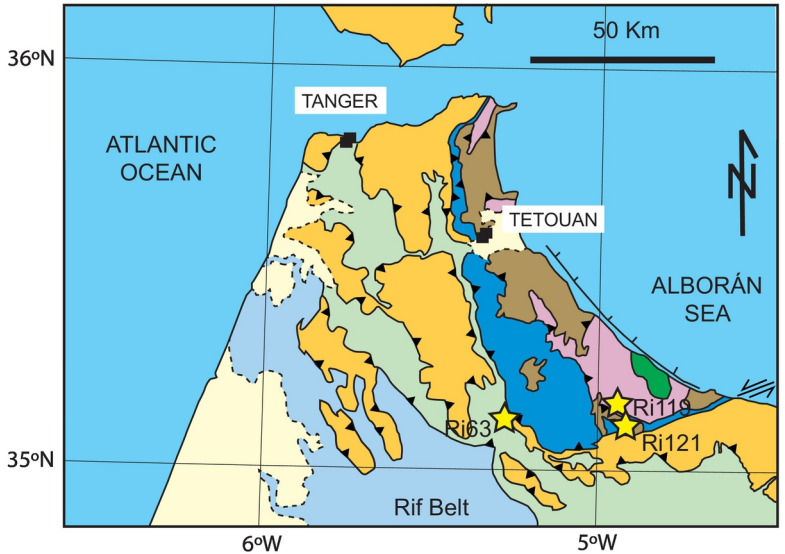
50 Km
36ºN
TANGER
ATLANTIC
OCEAN
TETOUAN
ALBORÁN
SEA
Ri119
Ri63
Ri121
35ºN
Rif Belt
6ºW
5ºW
Studied sample
AFRICAN PALEOMARGIN
External Rif
Olistostromes of the Pre-Rif Zone & Loukos and Rifian nappes
Tanger-Ketama unit (diagenesis-anchizone)
Maghrebian Flyschs Complex
Reverse fault
Normal fault
HINTERLAND
Internal Rif or Alborán Domain
Frontal units (“Dorsal Calcaire”)
Maláguide-Ghomaride Complex
Alpujárride-Sebtide Complex
Peridotites
Late Miocene-Quaternary sediments

Figure 3

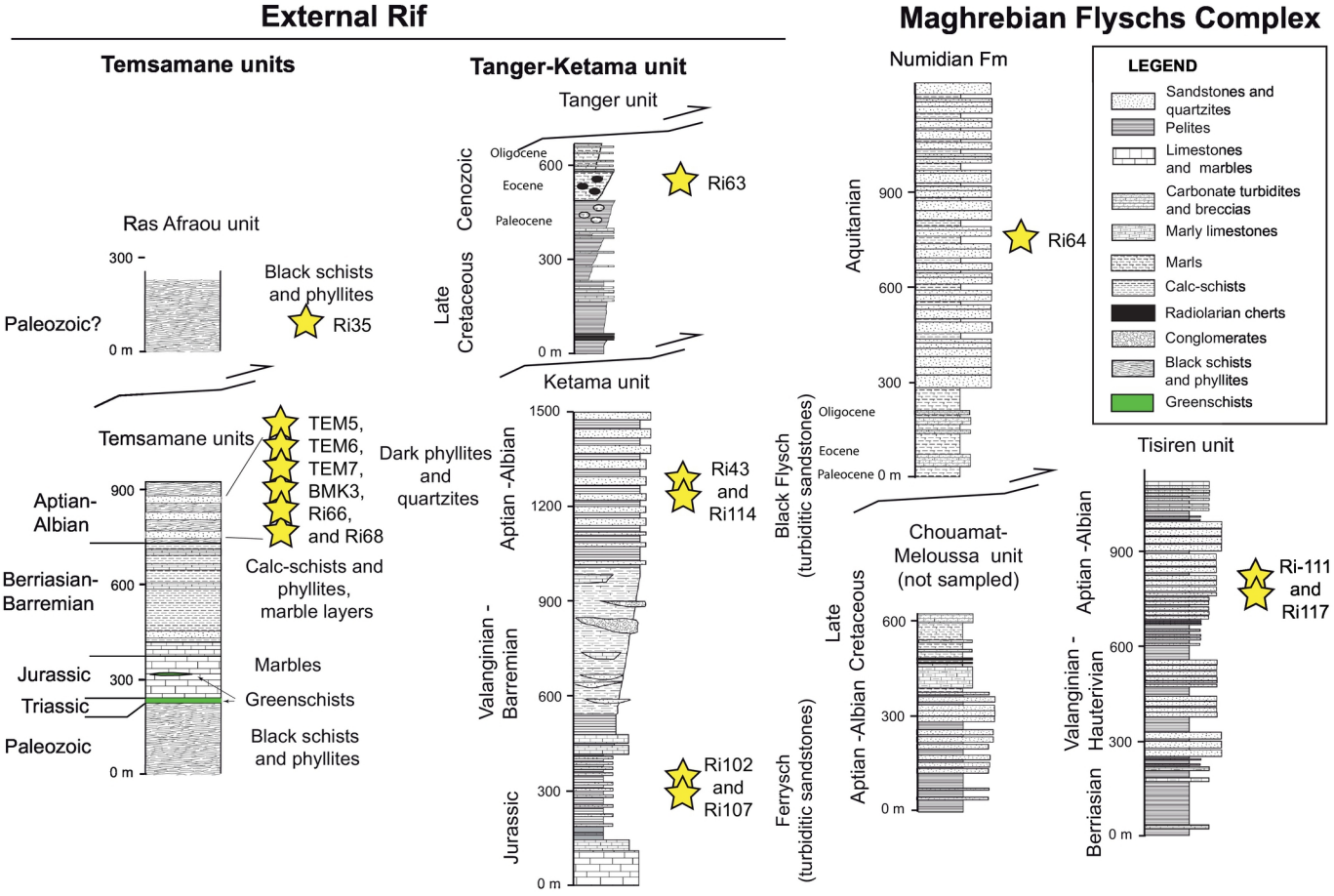
External Rif
Maghrebian Flyschs Complex
Temsamane units
Tanger-Ketama unit
Ras Afraou unit
Paleozoic?
300
0 m
Black schists and phyllites
Ri35
Tanger unit
Oligocene
Eocene
Paleocene
Cenozoic
Late Cretaceous
600
300
0 m
Ri63
Temsamane units
TEM5, TEM6, TEM7, BMK3, Ri66, and Ri68
Aptian-Albian
Berriasian-Barremian
Jurassic
Triassic
Paleozoic
900
600
300
0 m
Calc-schists and phyllites, marble layers
Marbles
Greenschists
Black schists and phyllites
Ketama unit
Dark phyllites and quartzites
Aptian -Albian
Valanginian - Barremian
Jurassic
1500
1200
900
600
300
0 m
Ri43 and Ri114
Ri102 and Ri107
Numidian Fm
Aquitanian
Oligocene
Eocene
Paleocene
900
600
300
0 m
Ri64
Black Flysch (turbiditic sandstones)
Chouamat-Meloussa unit (not sampled)
Late Cretaceous
Aptian -Albian
600
300
0 m
Ferrysch (turbiditic sandstones)
Tisiren unit
Aptian -Albian
Valanginian - Hauterivian
Berriasian
900
600
300
0 m
Ri-111 and Ri117
LEGEND
Sandstones and quartzites
Pelites
Limestones and marbles
Carbonate turbidites and breccias
Marly limestones
Marls
Calc-schists
Radiolarian cherts
Conglomerates
Black schists and phyllites
Greenschists

Figure 4

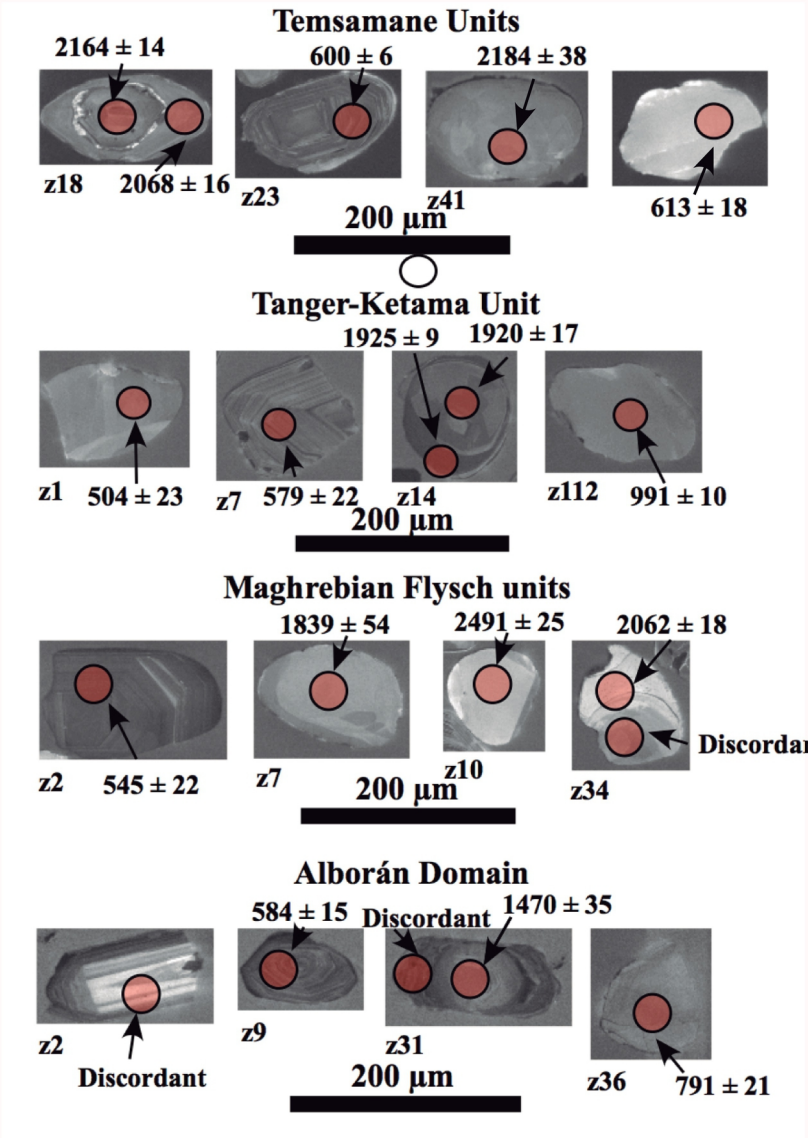
Temsamane Units
2164 ± 14
z18
2068 ± 16
600 ± 6
z23
2184 ± 38
z41
613 ± 18
200 µm
Tanger-Ketama Unit
1925 ± 9
1920 ± 17
z1
504 ± 23
z7
579 ± 22
z14
z112
991 ± 10
200 µm
Maghrebian Flysch units
1839 ± 54
2491 ± 25
2062 ± 18
Discordant
z2
545 ± 22
z7
z10
z34
200 µm
Alborán Domain
584 ± 15
Discordant
1470 ± 35
z2
Discordant
z9
z31
z36
791 ± 21
200 µm

Figure 5

TEMSAMANE UNITS

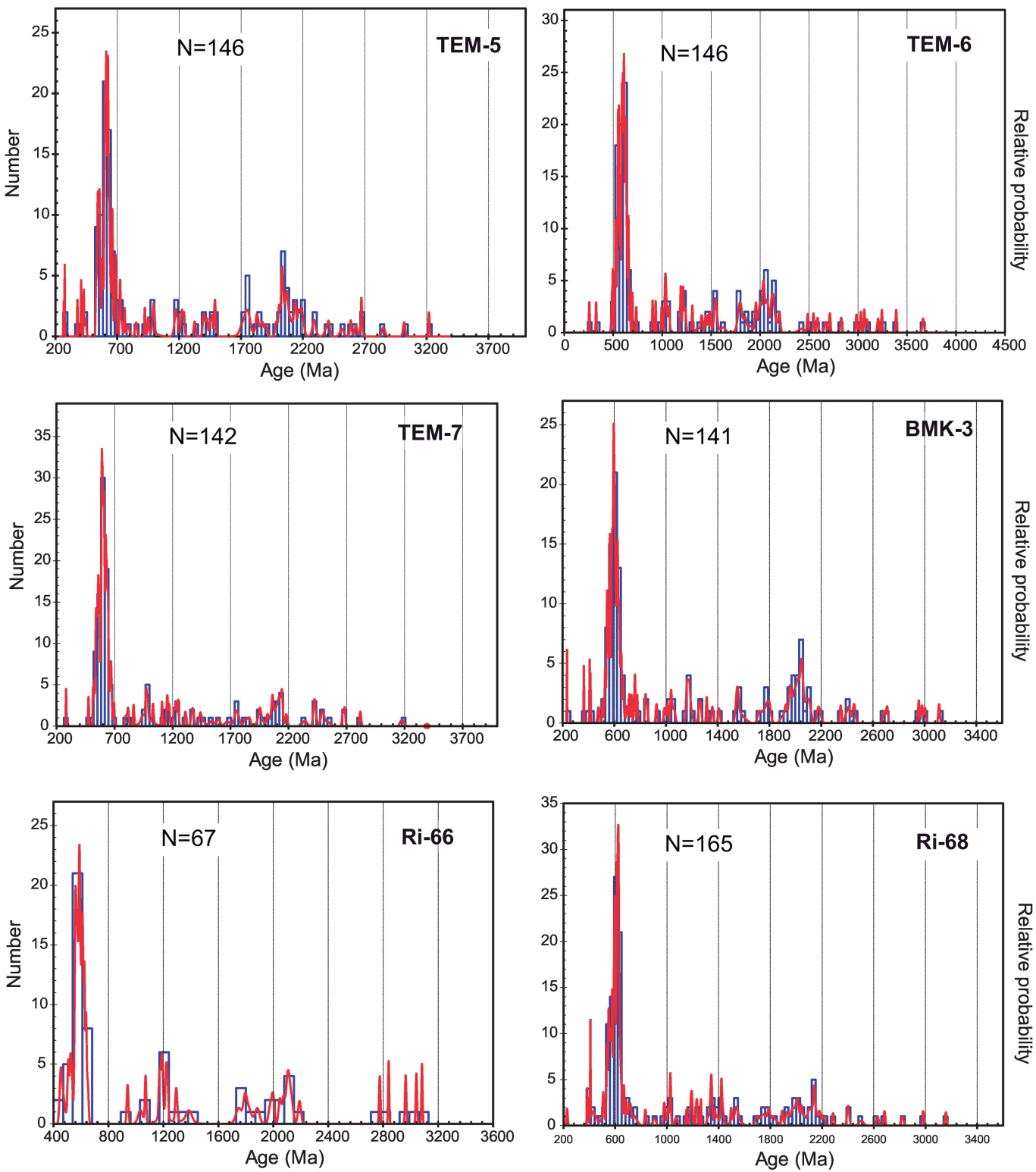

Figure 6

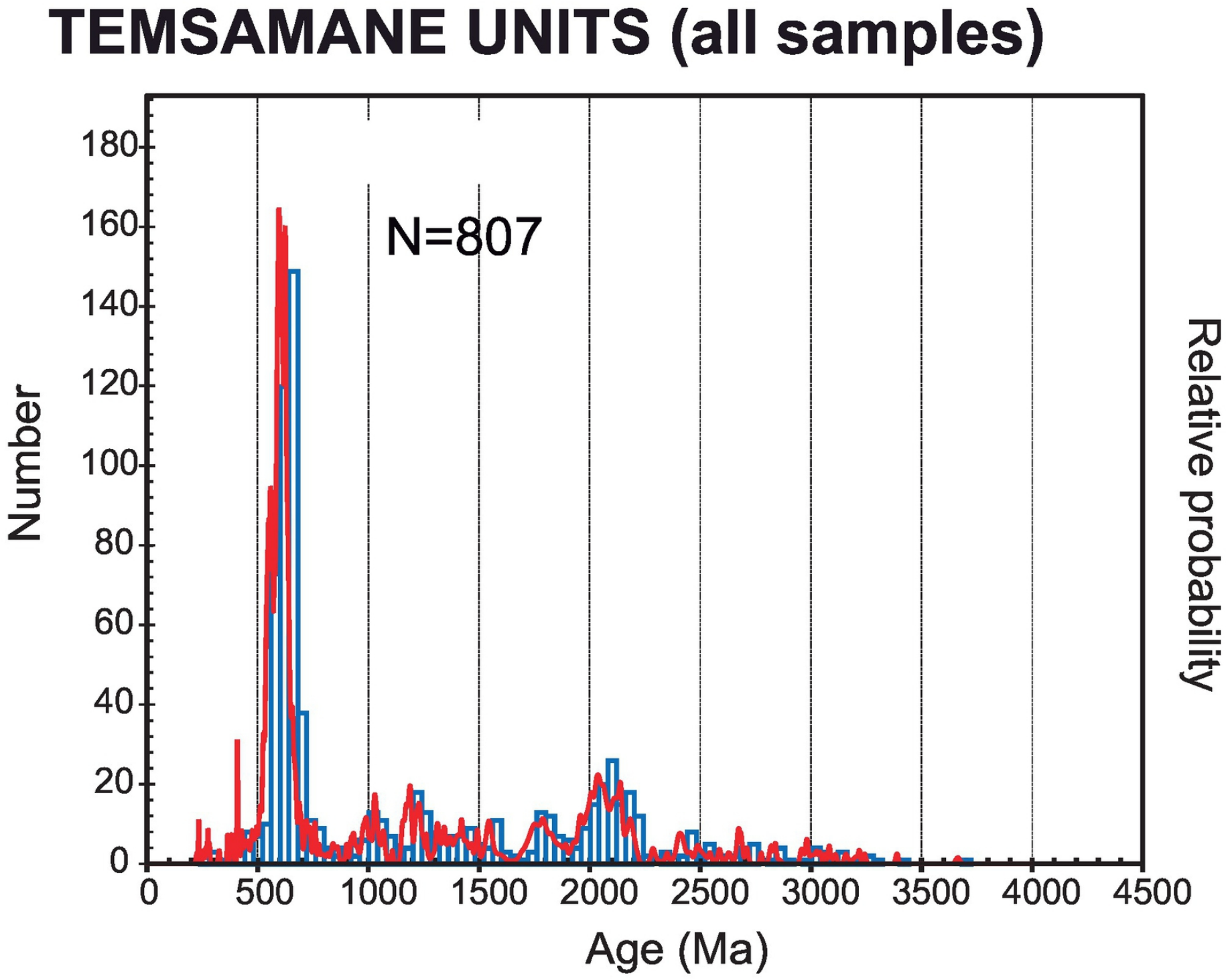
TEMSAMANE UNITS (all samples)
N=807
Number
Relative probability
Age (Ma)
0
20
40
60
80
100
120
140
160
180
0
500
1000
1500
2000
2500
3000
3500
4000
4500

Figure 7

RAS AFRAOU UNIT

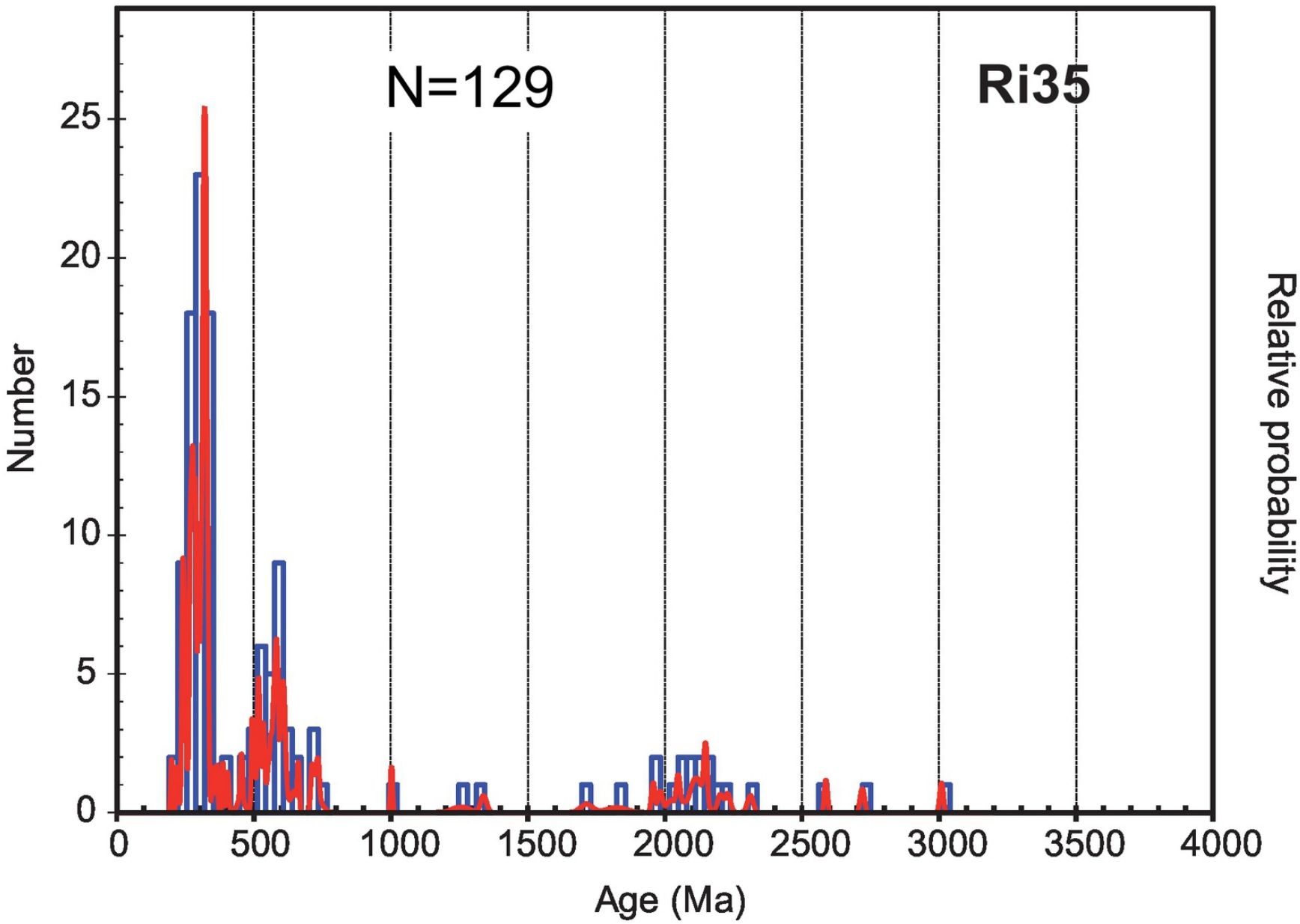

Figure 8

TANGER-KETAMA UNIT

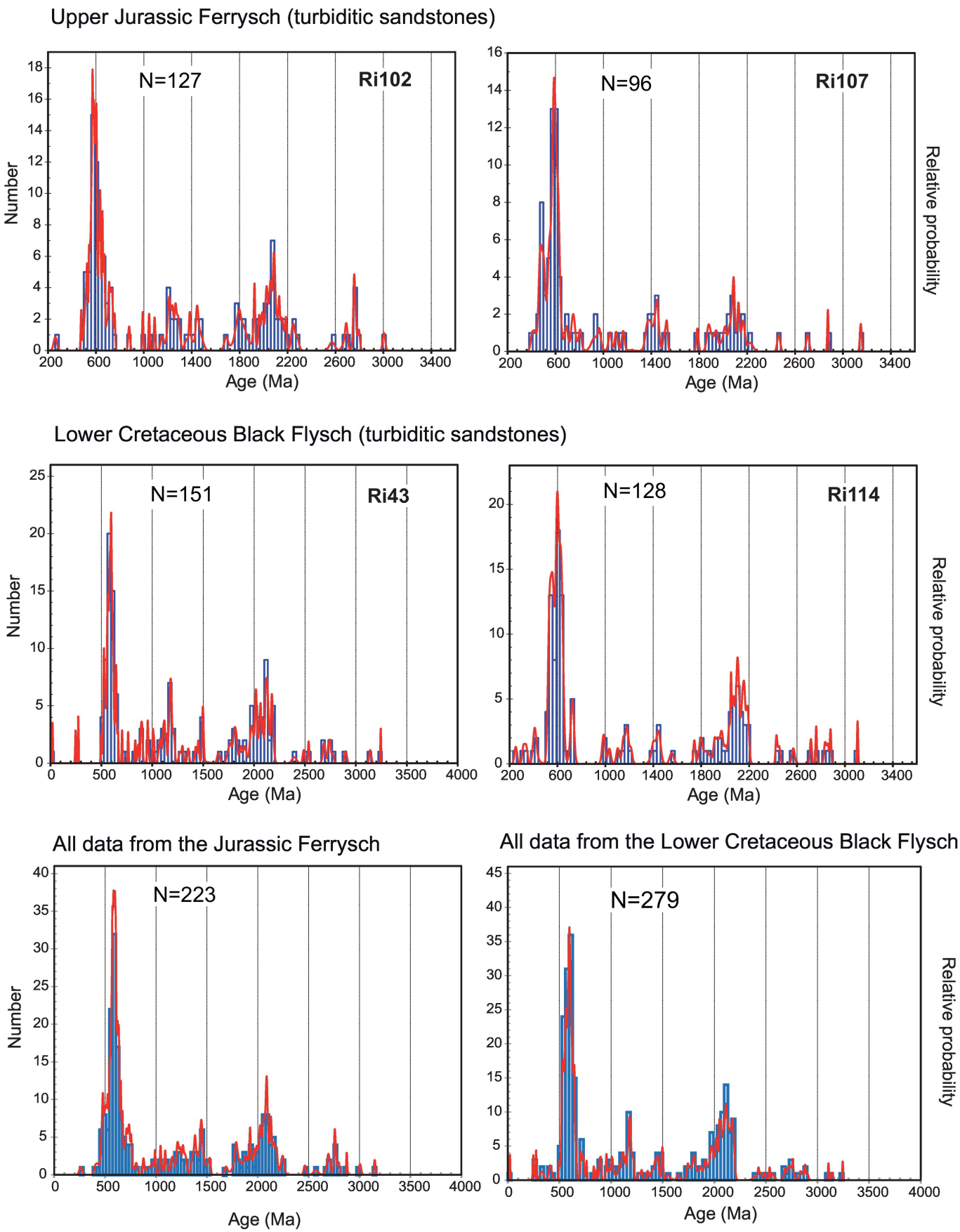

Figure 9

CENOZOIC SAMPLES

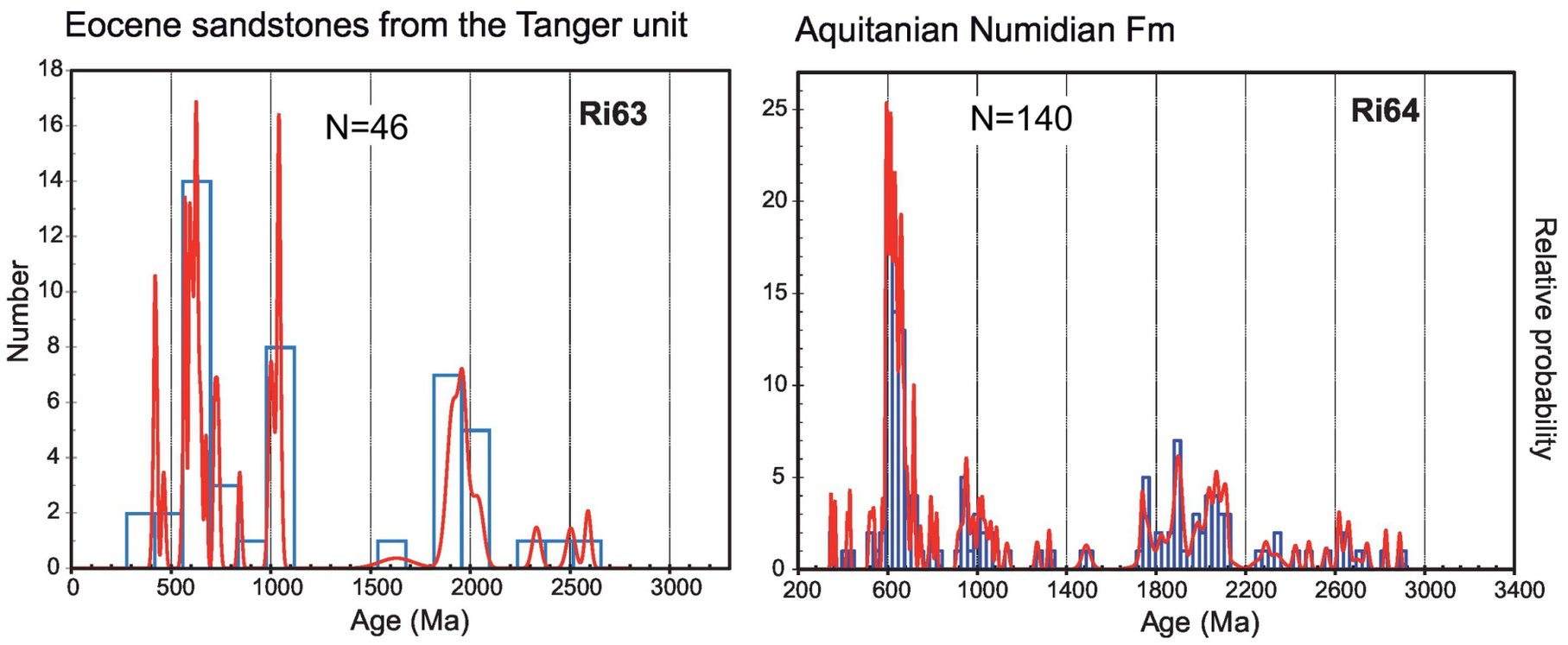

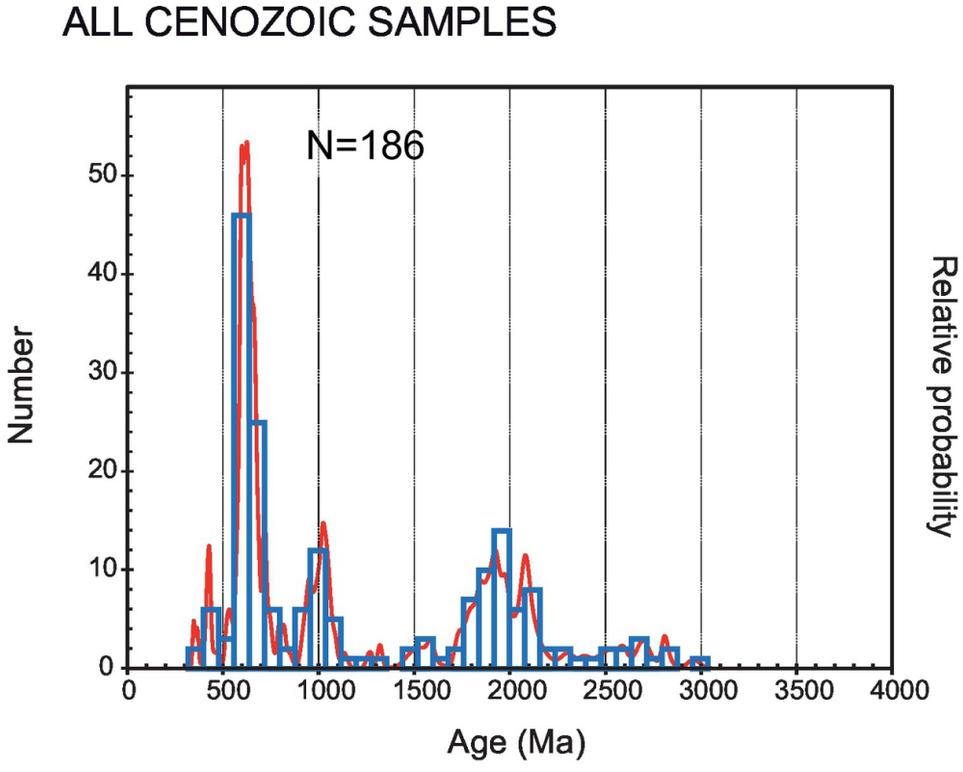

Figure 10

LOWER CRETACEOUS TISIREN FLYSCH

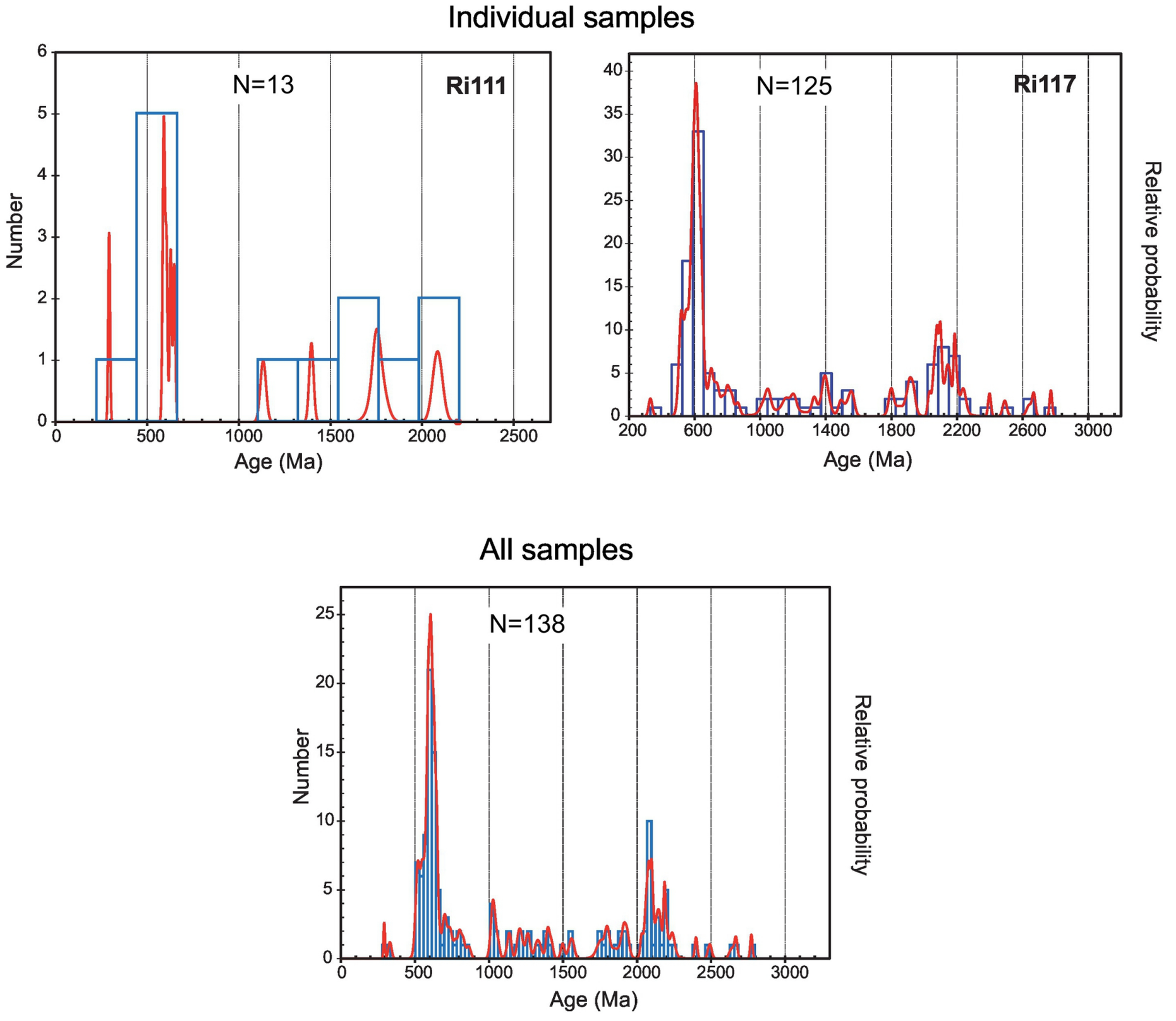

Figure 11

ALBORÁN DOMAIN

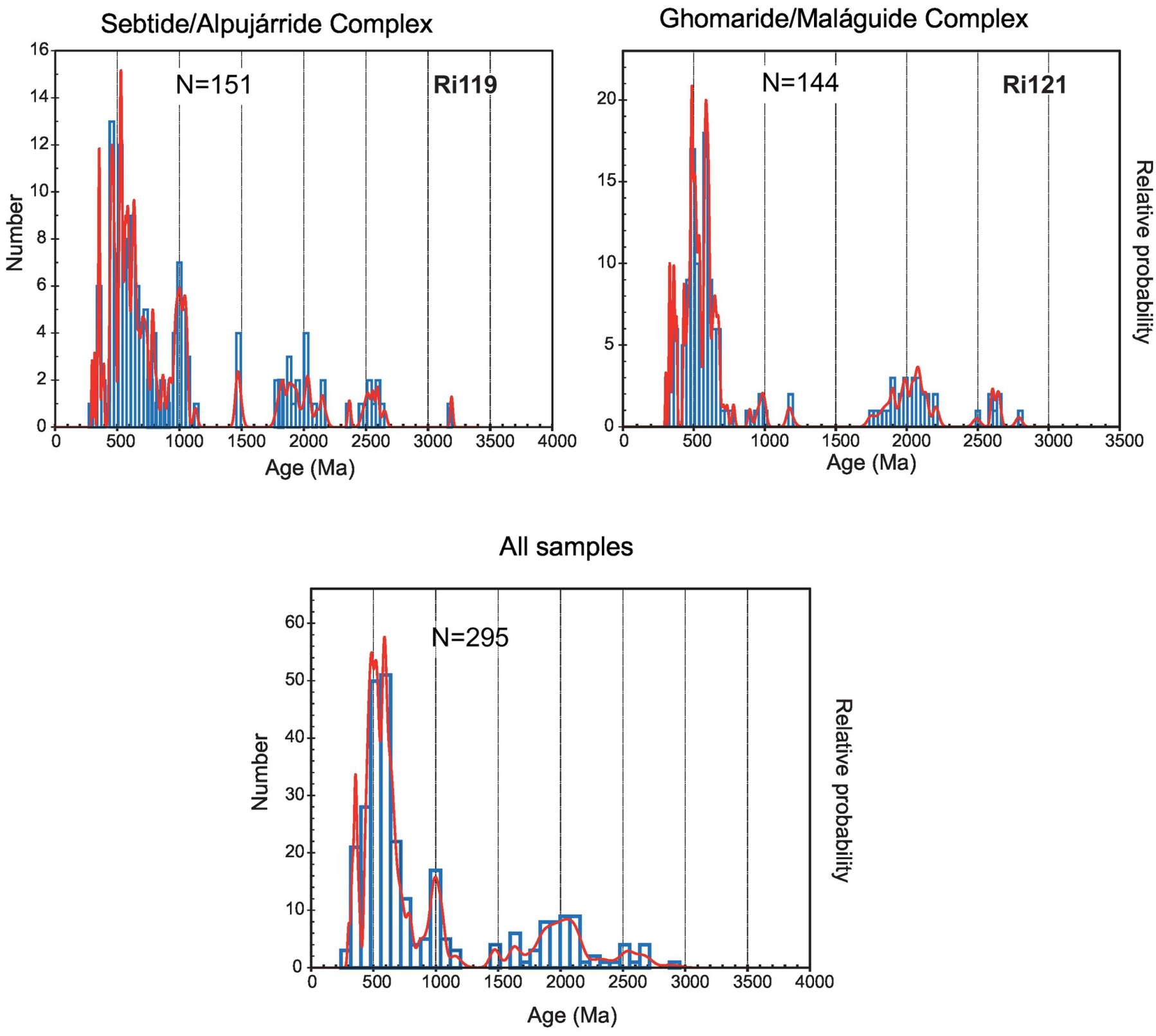

Figure 12

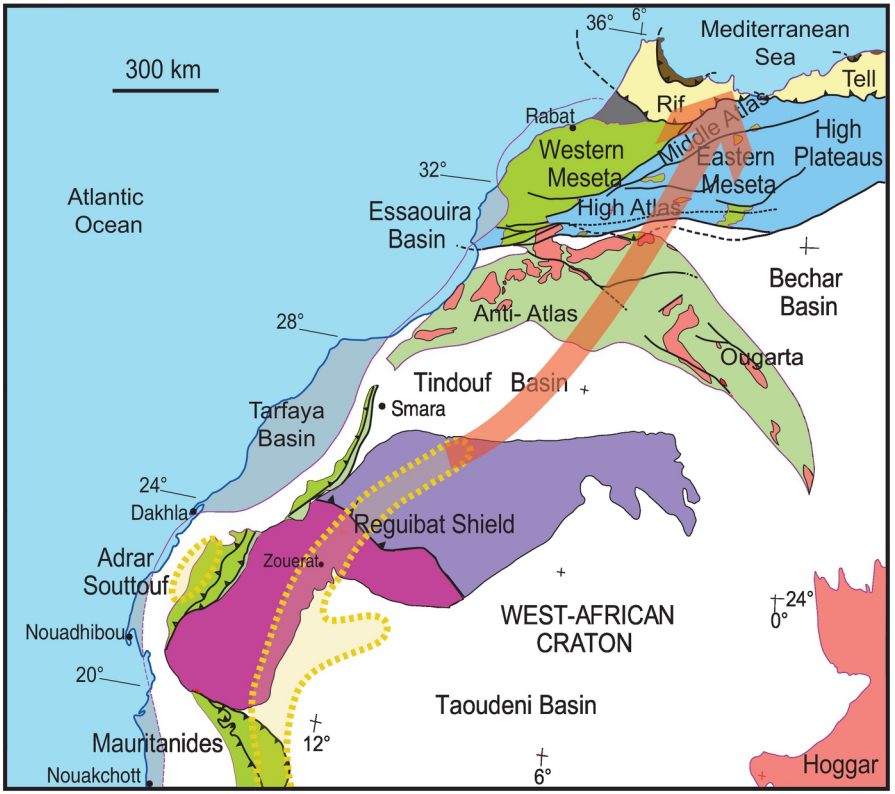

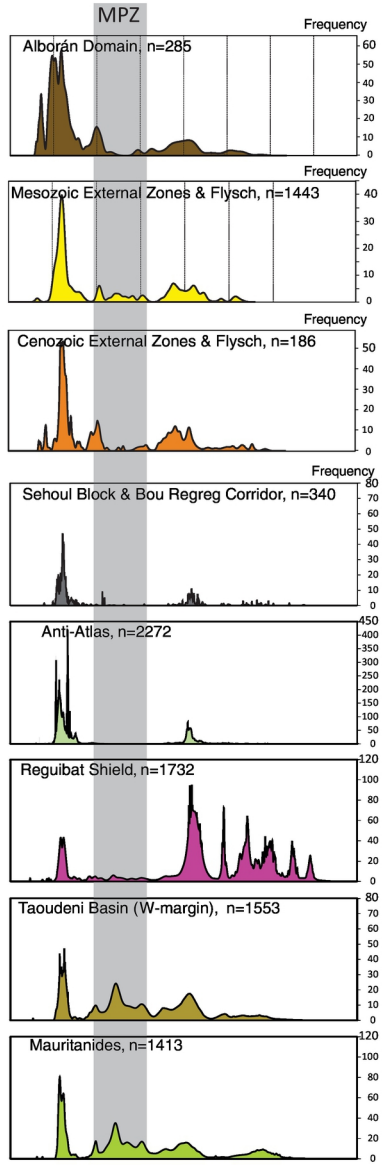

Archaean
Paleoproterozoic
Pan-African belt
Cratonic/ epicratonic basins
Atlantic coastal basins
Caledonian-Variscan belt
Sehoul block
Variscan foreland/ intracontinental belts
Atlas domain
Internal Maghrebides (Alborán Domain)
External Maghrebides
Areal distribution of sediment with significant Mesoproterozoic zircons (Gärtner et al., 2017)

Figure 13